Remote sensing techniques and stable isotopes as phenotyping tools to assess wheat yield performance: effects of growing temperature and vernalization

Fatima Zahra Rezzouk, Adrian Gracia-Romero, Shawn C. Kefauver, Nieves Aparicio Gutiérrez, Iker Aranjuelo, Maria Dolors Serret, José Luis Araus

PII: S0168-9452(19)30602-8

DOI: https://doi.org/10.1016/j.plantsci.2019.110281

Reference: PSL 110281

To appear in: *Plant Science*

Received Date: 7 May 2019

Revised Date: 16 September 2019

Accepted Date: 20 September 2019

Please cite this article as: Rezzouk FZ, Gracia-Romero A, Kefauver SC, Gutiérrez NA, Aranjuelo I, Serret MD, Araus JL, Remote sensing techniques and stable isotopes as phenotyping tools to assess wheat yield performance: effects of growing temperature and vernalization, *Plant Science* (2019), doi: https://doi.org/10.1016/j.plantsci.2019.110281

Remote sensing techniques and stable isotopes as phenotyping tools to assess wheat yield performance: effects of growing temperature and vernalization

Fatima Zahra Rezzouk[a,], Adrian Gracia-Romero[a], Shawn C. Kefauver[a], Nieves Aparicio Gutiérrez[b], Iker Aranjuelo[c], Maria Dolors Serret[a,], José Luis Araus[a*]

[a]*Section of Plant Physiology, University of Barcelona, Barcelona and AGROTECNIO (Center of Research in Agrotechnology), Lleida, Spain*

[b]*Agro-technological Institute of Castilla y León (ITACyL), Valladolid, Spain*

[c]*Instituto de Agrobiología (IdAB), Universidad Pública de Navarra-CSIC-, Multiva Baja, Navarra, Spain*

Corresponding author: Jose Luis Araus*

E-mail address: jaraus@ub.edu

Permanent address: Faculty of Biology, Avinguda Diagonal 643, 08028 Barcelona, Spain

Remote sensing techniques and stable isotopes as phenotyping tools to assess wheat yield performance: effects of growing temperature and vernalization

Fatima Zahra Rezzouk[a], Adrian Gracia-Romero[a], Shawn C. Kefauver[a], Nieves Aparicio Gutiérrez[b], Iker Aranjuelo[c], Maria Dolors Serret[a], José Luis Araus[a*]

[a]*Section of Plant Physiology, University of Barcelona, Barcelona and AGROTECNIO (Center of Research in Agrotechnology), Lleida, Spain*

[b]*Agro-technological Institute of Castilla y León (ITACyL), Valladolid, Spain*

[c]*Instituto de Agrobiología (IdAB), Universidad Pública de Navarra-CSIC-, Multiva Baja, Navarra, Spain*

Highlights:

- High temperature negatively affects wheat yield, particularly in winter genotypes
- Vegetation indices (VI) phenotype better genotypes in normal than in late planting
- Grain $\delta^{13}C$ and N content work well as phenotypic traits regardless of planting date
- Combination of VI and isotopes improved yield prediction for both planting dates.

Abstract

This study compares distinct phenotypic approaches to assess wheat performance under different growing temperatures and vernalization needs. A set of 38 (winter and facultative) wheat cultivars were planted in Valladolid (Spain) under irrigation and two contrasting planting dates: normal (late autumn), and late (late winter). The late plating trial exhibited a 1.5 ºC increase in average crop temperature. Measurements with different remote sensing techniques were performed at heading and grain filling, as well as carbon isotope composition ($\delta^{13}C$) and nitrogen content analysis. Multispectral and RGB vegetation indices and canopy temperature related better to grain yield (GY) across the whole set of genotypes in the normal compared with the late planting, with indices (such as the RGB indices Hue, a* and the spectral indices NDVI, EVI and CCI) measured at grain filling performing the best. Aerially assessed remote sensing indices only performed better than ground-acquired ones at heading. Nitrogen content and $\delta^{13}C$ correlated with GY at both planting dates. Correlations within winter and facultative genotypes were much weaker, particularly in the facultative subset. For both planting dates, the best GY prediction models were achieved when combining remote sensing indices with $\delta^{13}C$ and nitrogen of mature grains. Implications for phenotyping in the context of increasing temperatures are further discussed.

Keywords: Wheat; high temperature; vernalization; remote sensing; stable isotopes; yield prediction.

Abbreviations: CCI, chlorophyll/carotenoid index; CCiTUB, centres cientifics i tecnològics de la universitat de barcelona; CIELab, international commission on illumination lightness a* b*; CIELuv, international commission on illumination lightness u* v*; CT, canopy temperature; EVI, enhanced vegetation index; FIJI, fiji is just imageJ; GY, grain yield; GA, green area; GGA,

greener area; HSI, hue-saturation-intensity; HTPPs, high throughput phenotyping platforms; IR, infrared; IRMS, infrared mass spectrometer; ITACyL, instituto técnico y agrario de castilla y león; NDVI, normalized difference vegetation index; NIRS, near infrared spectrometers; NP, normal planting; VIs, vegetation indices; PRI, photochemical reflectance index; RGB, red-green-blue; TCARI/OSAVI, transformed chlorophyll absorption reflectance index/optimized soil adjusted vegetation index; TGW, thousand grain weight; UAV, unmanned aerial vehicle; VIF, variance inflation factor.

1. Introduction

Climate change is a prevalent concern that is already threatening food production and will even more so in the future, especially when addressing Mediterranean semi-arid climate regions [1–3]. Providing breeding and management practices are unchanged, annual rates of crop increase are more likely to decline as a response to drought periods and, even more importantly, to increases in temperature, including the frequency and strength of heat waves [4,5]. Therefore, efforts have to be harnessed into developing improved varieties that can be adapted to these rising challenges.

Wheat varieties have proven great adaptability to different agro-climatic regions [6]. Vernalization and photoperiod needs divide wheat genotypes into winter cultivars and spring (facultative) cultivars. The first category is usually sown in autumn or early winter [7,8], during which an exposure to low temperature (i.e. vernalization) is required in order to promote flowering. On the other hand, spring or facultative varieties do not require vernalization for flowering and thus, they can be more adapted to higher temperatures [8] and therefore they are more amenable for spring cultivation [7]. Besides the effect on floral induction, temperature also affects crop growth. High temperature accelerates the crop cycle and decreases the amount of accumulated photosynthesis, and the sinks (ear density and size in case of wheat), which subsequently reduces the final yield [9–11].

In recent years, the perception that crop phenotyping is a bottleneck that hinders breeding advances, has been widely recognized [12]. Presently, high throughput phenotyping platforms (HTPPs), placed at ground level or from the air (usually using unmanned aerial vehicles) have been developed to collect and handle accurately and in a non-invasive and fast way the large magnitude of information usually needed to properly phenotype crops in field conditions [13,14]. The main category of phenotyping techniques that may include HTPPs are categorized into remote (proximal) sensing and imaging. The most commonly deployed techniques deal with the use of spectroradiometrical and thermal sensors or imagers, together with an increasing use of conventional Red-Green-Blue (RGB) cameras [12,15,16]. The spectroradiometers measure different wavelength bands, within visible and near infrared regions of the spectrum, which allow the formulation of a wide range of vegetation indices informing on biomass [17,18], leaf area index [19,20], pigment content [21–23], nitrogen content [24,25], photosynthetic efficiency [26] and water status [26,27]. The thermal sensors and imagers measure the far infrared region of the spectrum informs on the plant canopy temperature and therefore of its water status [28,29]. Another category of remote sensing approaches is that derived from RGB images [12,30], with a wide range of vegetation indices being derived from different space colors which characterize the conventional images. It has been reported that frequently RGB indices work better than spectral indices in assessing differences in leaf color or green canopy area associated with genotypic performance, in optimal agronomical conditions as well as under different abiotic and biotic stress conditions [18,31]. Laboratory-category traits (i.e. analytical traits), may be also deployed for HTPPs [12]. When Mediterranean conditions are targeted, carbon and, to a lesser extent, nitrogen stable isotope compositions (or alternatively expressed as discrimination from the substrate) may be used as phenotyping tools, informing on the water regime and nitrogen metabolism conditions, respectively [32–34]. Several studies have highlighted the synergistic effect, in terms of quality

of plant characterization, when combining spectroscopy performance with the biophysical information provided through stable isotope composition [35,36].

The efficient use of the HTPPs, including the most adequate traits to measure, may be affected by the growing conditions. In that sense, as indicated above, one of the main environmental variables associated with climate change is temperature. The present study compares the performance of different phenotyping approaches under "current" temperature conditions (provided by a normal planting date) and high temperature conditions (provided by a late planting). Therefore, the heat stress conditions tested implies a constant higher temperature, besides a higher probability of experiencing a heat wave during the last part of the crop cycle. Another aspect related with increase in temperature is the potential altering effects on the pattern of flowering, associated with the lack of vernalization induction. To that end, we have concluded in the wheat panel winter (i.e. requiring vernalization) and facultative (less dependent on vernalization) semi-dwarf wheat cultivars. Different remote sensing techniques were implemented from ground and aerial levels, combined with the analyses of the stable carbon and nitrogen isotope composition of the flag leaves and mature grains.

2. Materials & methods

A set of 36 post green revolution (i.e. semidwarf) bread wheat commercial cultivars (*Triticum aestivum* L.) were evaluated altogether with other 2 durum wheat cultivars (*Triticum turgidum* L. ssp. *durum* (Desf.) Husn.) (Table 1). In order to assess vernalization effects on final production and yield components, cultivars were separated into winter (27) and facultative genotypes (11). Field trials were carried out in the Experimental Station of Zamadueñas (41º 39´ 8´´ N and 4º 43`24`` W, 690 m.a.s.l.); of the Instituto Técnico y Agrario de Castilla y León (ITACyL) in Valladolid (Spain) (Fig. 1). Temperature effects were investigated through implementing trials under contrasting planting dates: a normal planting (December 2nd, 2016), followed by a late planting (February 10th, 2017). The late planting trial (and specifically the facultative cultivars) caught up with the development of the facultative and winter genotypes of the normal planted trial around 90 days after sowing, corresponding to the heading-anthesis stages. Patterns of precipitation, temperature (average, minimum and maximum) and photoperiod throughout the crop season are displayed in Fig. 2. Accumulated precipitation from planting to maturity during the crop cycle were 129 mm and 89 mm, for the normal and late planting respectively. In order to restrict environmental stress factors to temperature, both trials were grown under support irrigation, supplied with periodical sprinkler irrigation totaling 60 mm during normal planting, and 140 mm during late planting. Fertilizers were applied as recommended; it consisted for both trials in 300 kg ha^{-1} of basic dressing in the form of 8-15-15 (N-P-K) before seeding, ensued with a twofold partitioning of 300 kg ha^{-1} of Nitrosylsulphuric acid (NSA, 27%) as top dressing during stem elongation and booting stages. Phytosanitary control included the spraying of herbicides (*Axial* and *Amadeus*, *Syngenta*), fungicide (*Karate Zeon*, *Syngenta)* and pesticide (*Prosaro*, *Bayer*) at the recommended rates during booting (late planting) and heading (normal planting) stages. For both trials, the experimental design was fully randomized with three replications (individual plots) per genotype, totaling for each trial 114 plots (81 and 33 plots per winter and facultative genotypes, respectively). Plots were 6 m long and 1.5 m wide, with 7 rows sown 20 cm apart (totaling 9 m^2 per plot). During early grain filling flag leaves were sampled, and by physiological maturity number of spikes per square meter was evaluated together with grain number per spike and thousand grain weight, for genotypes in normal planting, and only number of spikes per square meter in late planting. For both trials, maturity was reached the second half of June. Then, plots were harvested mechanically on July 20th, 2017 for both trials and yield assessed.

2.1 Ground and aerial remote sensing

Plots were evaluated at ground level using a Red-Green-Blue (RGB) camera, an infrared thermometer and a spectro-radiometer. Aerial images were obtained during the same visits as ground data using an Unmanned Aerial Vehicle (UAV) (Drone Mikrokopter OktoXL 6S12, Moormerland, Germany), controlled manually and flying at an altitude of 50 m, carrying a digital RGB camera just before solar noon in the first flight, and thermal and multispectral cameras within one hour of solar noon in the second flight. For normal planting, the range of heading dates for the whole set of genotypes was about 10 days, while in the late planting the range was larger (around 30 days) due to the delay in the reproductive stage experienced by the winter genotypes. During the first date of measurements (middle-May), the whole set of genotypes for the normal planting and the subset of facultative genotypes for the late planting were at late heading. During the second visit (second week June), the whole set of genotypes for the normal planting and the subset of facultative genotypes for the late planting were in the second half of grain filling.

2.1.1 Canopy temperature

Measurements of canopy temperature (CT) at ground level were carried out during both visits using an infrared (IR) thermometer (PhotoTemp^{TM} MXS^{TM}TD Raytek$^{®}$, California; USA), pointed towards plants leaves at a distance of 80 cm approximately, while having the sun towards the rear. For aerial thermal images, a FLIR Tau2 640 was used (FLIR Systems, Nashua, NH, USA) with a VOx uncooled microbolometer, equipped with a TEAX Thermal Capture model (TeAx Tecnology, Wilnsdorf; Germany) for recording thermal frames of full resolution (640×520 pixels at 20 frames per second).

2.1.2 RGB images

RGB images (one per plot) were taken from ground holding a Sony ILCE-QX1 (Sony Europe Limited, Brooklands; United Kingdom), digital camera of 20.1 megapixel resolution, equipped with 23.2 mm × 15.4 mm sensor size (type CMOS Exmor HD) and using 16 mm focal lens and an exposure time of 1/60 seconds. Images were captured zenithally at 80 cm above the plant canopy, focusing near the center of each plot, and then saved in JPEG format for later analysis. The ground sample distance (GSD) of the images captured was 0.021 cm/pixel, and the area captured in the image corresponded to 0.89 m^2. For aerial data assessment, the RGB used camera was a Lumix GX7 (Panasonic, Osaka; Japan), a digital mirrorless camera of 16.0 megapixel resolution with an image sensor size of 17.3×13.0 mm (type Live MOS), using a 20 mm focal lens with an exposure time of 1/8000 seconds. The GSD of the aerial images for a flight at 50 m altitude was 0.941 cm/pixel, and the area captured in the image corresponded to 1404.55 m^2. In practical consideration, mirrorless cameras provide equal imaging capacities for agricultural applications than traditional cameras in a more compact and lightweight body, which promote their flexible application in the field or mounted on a UAV.

2.1.3 Multispectral information

The normalized difference vegetation index (NDVI) was measured at ground (NDVI.g) on individual plots using a GreenSeeker (Trimble, Sunnyvale, CA, USA), a hand held spectroradiometer with active self-illuminated sensor in red (660 ± 10 nm) and near infrared (780 ± 15 nm) wavelengths [37]. The NDVI was measured by skimming the sensor across each plot, at a constant height of 60 cm while maintaining a perpendicular position from above the canopy [38]. At this distance, the sensor field of view emits a strip of 61 cm long and 1.5 cm thick.

Multispectral aerial images were acquired using a Tetracam micro-MCA (Tetracam Inc., Chatsworth, CA; USA). The Tetracam camera consists of eleven independent image sensors and optics each, using configurable filters of center wavelengths and full-width half-maximum bands with: 450 ± 40, 550 ± 10, 570 ± 10, 670 ± 10, 700 ± 10, 720 ± 10, 780 ± 10, 840 ± 10, 860 ± 10, 900 ± 20 and 950 ± 40 nm. In addition, the camera possesses one sensor dedicated to calibration (Incident Light Sensor, ILS), which provides band-by-band reflectance calibration in real-time, correcting the 11 bands to reduce atmospheric effects to at-sensor reflectance. The multispectral camera is equipped with rolling shutter sensors system, and captures 15.6 megapixels of image data that are transferred to twelve separate flash memory cards [17]. Every UAV flight included between 20-30 image capture moments, each consisting of the 12 images representing the 11 spectral bands and ILS of the sensor, which recorded data every 5 s.

2.1.4 Image processing

Pre-processing was required for multispectral and thermal images. Multispectral images were spatially aligned and radiometrically calibrated using PixelWrench 0.2 version 1.2.2.2 (Tetracam, Chatsworth, CA, USA) and exported as TIFF files. Whereas thermal frames were stacked to raw 16-bit TIFF format (temperature values expressed in Kelvin x 10000) using the ThermoViewer software (v1.3.13) by TEAX (TeAx Technology, Wilnsdorf, Germany). Therewith, RGB, thermal and multispectral images were 3D-reconstructed using Agisoft Photoscan Pro (Agisoft LLC, St. Petersburg, Russia, www.agisoft.com) [39]. This later overlaps up to 30 images (with at least 80% overlap) and removes UAV flight effects to produce accurate ortho-mosaics. Afterwards, regions of interest (plots) were cropped and processed using the MosaicTool software (Prof. Shawn C. Kefauver, https://integrativecropecophysiology.com/software-development/mosaictool/, https://gitlab.com/sckefauver/MosaicTool/, University of Barcelona, Barcelona, Spain) integrated as a plugin for the open source image analysis platform FIJI (Fiji is Just ImageJ; http://fiji.sc/Fiji) [40].

Extracted RGB vegetation indices collected from both ground and aerial platforms were obtained using an updated version of the original Breedpix 2.0 software [41], which is a tool for fast calculation of pictures-based vegetation indices (Pic-VIs), adapted to JAVA8 and integrated as MosaicTool plugin within FIJI [40]. RGB indices are related to different color properties and based either on the average color of the entire image on the proportion of green pixels over the total number of pixels in the full image. CIELab and CIELuv color space models were defined by the CIE (Commission Internationale de l'Eclairage; the International Commission on Illumination) as the simultaneous contrast of green with red colors (CIELab), and yellow with blue colors (CIELuv) [42]. Both models operate similarly albeit on separate spectrums, and include lightness component (L*), a* and b* dimensions for CIELab, and u* and v* coordinates for CIELuv. The indices a* and u* represent the green to red spectrum, where red is linked to positive values and green to negative ones; whereas b* and v* express the blue to yellow spectrum, where yellowish pixels are related to positive values and conversely, bluish pixels to negative ones. HSI color space, referring to the components Hue, Saturation and Intensity. This color space model describes saturation as the pure (chroma) concentration when diluted with white color, and intensity as the achromatic measurement of the reflected light. Regarding Hue, it is described as the chroma traversing the visible spectrum in the form of an angle between 0° and 360°, where 0° and 360° are decrypted into red, 60° into yellow, 120° into green and 180° into cyan. Derived from the Hue, the indices Green Area (GA) and Greener Area (GGA) were described as the fraction area presented by green pixels in the image, and which Hue ranges from 60º to 180º (GA) and from 80º to 180º (GGA). While GA gives a broader perception to canopy greenness, GGA excludes yellowish green pixels [31,41]. The current study was limited to the parameters (Hue, a*, b*, GA and GGA), as the best performed RGB indices.

Multispectral indices were formulated using a custom FIJI macro code built into the MosaicTool software (University of Barcelona, Spain). The macro operates through measuring the mean value

of the plot image of each band to calculate the following indices: Normalized Difference Vegetation Index (NDVI), Enhanced Vegetation Index (EVI), Photochemical Reflectance Index (PRI), Chlorophyll/Carotenoid Index (CCI), Transformed Chlorophyll Absorption Index (TCARI), and the TCARI/OSAVI index ratio . Likewise, aerial CT was acquired using a custom batch processing macro function in FIJI that converts 16-bit images (in Kelvin x 10000) to 32-bit images (in Celsius) [40]. Further information regarding the selected RGB and multispectral indices is summarized in Table 2. These indices represent a selection of the classic reference indices, the most relevant, enhanced, optimized, and transformed index variations and the best capacity of our Tetracam multispectral sensor to measure different traits separately.

2.2 Carbon and nitrogen stable isotope composition

Flag leaves, sampled during grain filling (coinciding with the second measuring data), and mature grains, collected at harvest, were dried at 60 ºC for a minimum of 48 hours finely ground using a grinder machine (Mixer Mill MM 400; Retsch GmbH, Haan; Germany), and then weighed in tin capsules (approximately 1 mg) for further analysis of the carbon and nitrogen stable isotope signatures and the total nitrogen and carbon contents. Stable isotope values were expressed in composition (δ) units, as the deviation of the isotopic composition of the material from the standard. Thus, the carbon and nitrogen isotopic compositions ($\delta^{13}C$ and $\delta^{15}N$) were expressed as:

$$\delta^{13}C \text{ or } \delta^{15}N\ (‰) = [(R_{sample}/R_{standard}) - 1] \times 1000$$

Where the $^{13}C/^{12}C$ and $^{15}N/^{14}N$ ratios of the sample are notated as $\delta^{13}C$ and $\delta^{15}N$ and expressed in ‰, whereas $R_{standard}$ is the molar abundance ratio of the secondary standard calibrated against the primary standard Pee Dee Belemnite ($\delta^{13}C$) and N_2 from air ($\delta^{15}N$) [43]. Different secondary standards were used for carbon (IAEA-CH_7, IAEA-CH_6 and IAEA-600, and USGS 40) and nitrogen (IAEA-600, N_1, N_2, NO_3, UREA and Acetanilide) isotope analyses. Analytical precision of the $\delta^{13}C$ and $\delta^{15}N$ analyses were 0.1‰ and 0.3‰, respectively. Total carbon and nitrogen contents in flag leaves and grains were expressed as the percentage (%) of total carbon and nitrogen on dry matter basis. Isotopes and elemental analyses were performed employing an elemental analyzer operating in a continuous flow mode with a mass spectrometer (Delta C IRMS; ThermoFinnigan, Bremen; Germany), at the Scientific and Technical facilities of the University of Barcelona (Centres Científics i Tecnològics de la Universitat de Barcelona (CCiTUB)).

2.3 Statistical analysis

Analysis of variance (ANOVA) was performed using SPSS 20 (IBM SPSS Statistics 20, Inc., Chicago, IL; USA), to test the effects of planting date (normal vs late planting), genotypes attitude (winter vs facultative) and genotypic differences per subset (winter or facultative) and within each subset, for all parameters evaluated. The same analysis of variance was run also using days to heading (DTH) as a covariable to remove the effect of phenology. A bivariate Pearson correlation was used operating with the same statistical package SPSS 20 to evaluate relationships between all analytical traits and GY. Yield prediction was assessed by implementing stepwise multiple regression models within each treatment, where a multicollinearity level was controlled by setting a maximum variance inflation factor (VIF) at 10. Graphs were created using the softwares SigmaPlot 10.0 (Systat Software Inc, California; USA) and the open source software R and RStudio 1.0.44 (R Foundation for Statistical Computing, Vienna, Austria).

3. Results

3.1 Effect of planting date and genotype attitude on yield and agronomical components

Effects of planting date ($P < 0.001$) and genotype attitude ($P < 0.05$) on grain yield (GY) were significant (Table 3). Means of GY and the number of spikes per square meter (spikes m^{-2}), as well as days to heading were greater in the normal planting compared to late planting regardless of the genotypic attitude (winter or facultative). Winter cultivars exhibited higher GY, spikes m-2, grains spike-1 and days to heading and lower thousand grain weight (TGW) and grain weight spike-1 than the facultative genotypes in the normal planting. However, in late planting, days to heading was the only trait where genotypic attitude had a significant effect, with facultative cultivars reaching heading in average three weeks earlier than winter cultivars. Moreover, heading in the winter cultivars was not synchronized. For a given cultivar, the culms did not extrude the ears simultaneously but rather extended in time. Interaction between planting date and genotypic attitude was significant for GY and days to heading. In normal planting genotypic differences were also significant for GY and TGW within each subset of cultivars (winter and facultative), and with grain weight $spike^{-1}$ and spikes m^{-2} in winter cultivars. In late planting, genotypic differences were found for GY in winter cultivars, and for spikes m^{-2} within facultative ones (Supplemental Table 1).

3.2 Effect of planting date and genotypes attitude on RGB and multispectral indices

Remote sensing techniques were implemented during two consecutive visits (coinciding roughly with late heading and the second half of the grain filling). During heading, all the aerial RGB indices along with the multispectral NDVI.g were affected by planting date (Table 4). RGB vegetation indices were significantly lower in normal planting compared to late planting except for the Hue.a and GGA.a, while NDVI.g exhibited an opposite behavior. Among these indices solely the Hue.a, GA.a and NDVI.g were affected by genotypic attitude and its interaction with planting date. Furthermore, and within normal planting, b*.a, GA.a and GGA.a and the multispectral index TCARIOSAVI.a were higher across facultative genotypes than within winter ones. However, the RGB and multispectral indices assessed at ground level failed to separate between genotypic attitudes (Table 4). In late planting, no significant effect was revealed between winter and facultative genotypes except for the RGB index a*.a and NDVI.g (Table 4), while ground RGB indices and aerial multispectral indices were not assessed. In normal planting, genotypic differences within both subsets (winter and facultative) were shown for the RGB index Hue.g, and for most aerially assessed RGB indices (except a*.a), while genotypic differences within the winter set of genotypes also existed for NDVI.g, the RGB indices a*.g, b*.g, GGA.g and a*.a. In late planting, solely NDVI.g within facultative cultivars exhibited genotypic differences, while no genotypic effects were found for other indices within the subsets of winter and facultative genotypes (Supplemental Table 2).

The grain filling stage (assessed during the second visit) revealed significant planting date and genotypic attitude effects for almost all RGB and multispectral indices derived from both ground and aerial platforms, whereas the interaction effect between these factors was only significant for some RGB indices (Hue.g, a*.g, GGA.g and GA.a). Regardless of being acquired at ground or from the aerial platform, multispectral indices PRI and NDVI and RGB indices GA and GGA increased significantly in late planting compared to normal planting. Moreover, and in both planting dates, RGB and multispectral vegetation indices recorded significantly higher values in winter genotypes compared to facultative ones (Table 4). At the normal planting and within both subsets of cultivars, genotypic differences existed for the multispectral index (EVI.a), while genotypic differences for the RGB indices b*.g and the GGA.a were found only across the winter subset. In late planting, genotypic differences were significant within both winter and facultative genotypes regarding RGB and multispectral indices (Hue.g, a*.g, b*.g and NDVI.g), while GA.g and GGA.g were only significant within facultative genotypes (Supplemental Table 2).

3.3 Effect of planting date and genotypes attitude on water regime and nitrogen status parameters

In both heading and grain filling canopy temperature (CT) assessed from ground (i.e. at single plot level) was affected significantly by planting date and genotypic attitude, while interaction for these factors occurred during grain filling only. Significant differences between genotypic attitudes were well evident in normal planting during heading and in the late planting during grain filling, where facultative genotypes exhibited higher CT.g than winter ones. Likewise, CT.a was significantly higher in facultative genotypes than winter ones in both phenological stages when measured in normal planting date (Table 5). Moreover, significant genotypic differences were shown within facultative genotypes at heading in both planting dates, but were not evidenced during grain filling (Supplemental Table 3).

Nitrogen content (N) and carbon isotope composition ($\delta^{13}C$) of flag leaves and grains, together with nitrogen isotopic composition ($\delta^{15}N$) of flag leaves were significantly affected by planting date and genotypic attitude, while carbon content in grains was only affected by planting date. A significant interaction between planting date and genotypes attitude was found only for N_{grain} and $\delta^{13}C_{leaf}$ (Table 5). In both flag leaves and grains, N and $\delta^{13}C$ were higher in normal planting compared with late planting. Furthermore, winter genotypes exhibited higher N_{leaf} and lower $\delta^{13}C_{leaf}$, N_{grain} and $\delta^{13}C_{grain}$ than facultative genotypes in normal planting, and higher N_{leaf} and $\delta^{13}C_{leaf}$ in late planting. In normal planting genotypic differences were shown for N_{grain} within both subsets (winter and facultative), and for $\delta^{13}C_{leaf}$ and $\delta^{15}N_{leaf}$ and $\delta^{15}N_{grain}$ only within facultative cultivars. In late planting, genotypic differences were only found for $\delta^{13}C_{leaf}$, $\delta^{13}C_{grain}$ and N_{grain} within winter genotypes (Supplemental Table 3).

3.4 Effect of phenology on grain yield and phenotypical traits

For grain yield, agronomical components and all the phenotypical traits assayed, ANOVA was also run using days to heading as a covariate, to remove the effect of phenology. In this context, planting date did not have a significant effect on GY and number of spikes m^{-2}. Moreover, phenology significantly affected GY, number of spikes m^{-2}, the traits informing on water status (CT and heading and grain filling, and $\delta^{13}C$ of the flag leaf and mature grains) and most of the remote sensing vegetation indices. Nevertheless, the effect of genotype attitude (winter versus facultative) was still significant for GY, number of spikes m^{-2}, $\delta^{13}C_{leaf}$ and $\delta^{13}C_{grain}$ and N content of the grain, as well as most of the RGB vegetation indices measured during grain filling.

3.5 Performance of yield components assessing GY within planting dates and genotypic attitudes

Correlation coefficients of the linear regressions of GY against days to heading and agronomical yield components using genotypic means are presented (Table 6). In the case of normal planting, days to heading correlated positively and thousand grain weight negatively against GY only when combining both categories of genotypes. In the late planting, GY related negatively to days to heading and positively to spikes m-2 (the only yield component measured) across both set of genotypes.

3.6 Performance of RGB and multispectral indices assessing GY within planting dates and genotypic attitude

In the normal planting, during heading and using genotypic means (Table 7), all aerially assessed RGB vegetation indices together with the multispectral TCARIOSAVI.a correlated with GY across both subsets of genotypes, while the ground-assessed RGB indices and the rest of multispectral indices did not correlate. As per genotypic attitude, the RGB indices a*.a, GA.a and GGA.a correlated within winter genotypes, while the Hue.a and multispectral indices EVI.a and TCARIOSAVI.a correlated with GY within facultative ones. In the late planting however, only the RGB parameters a*.a and b*.a correlated against GY; in this case across all genotypes as well as within winter genotypes.

During grain filling, for normal planting, all RGB and multispectral indices assessed at ground and aerially were significantly correlated against GY across both subsets of genotypes combined (Table 7). Regarding genotypic attitude however, only the RGB index a*.a and the multispectral EVI.a correlated with GY within facultative genotypes, and no correlation existed within winter ones. In the late planting, only the RGB indices b*.g and a*.a, together with multispectral indices EVI.a and CCI.a correlated with GY across both categories of genotypes as well as (except for b*.g) within winter genotypes only. No other vegetation index correlated with GY within the winter and facultative subsets of genotypes.

3.7 Performance of canopy temperature, stable isotope signatures and N content assessing GY within planting dates and genotypes attitude

In the normal planting (and except for ground-assessed CT at heading), CT correlated negatively with GY across the whole set of genotypes in the normal planting. In the late planting negative correlations were achieved only at heading and this index also correlated negatively with GY within the winter subset of genotypes. No other correlation between CT and GY within each of the two subsets of genotypes were recorded (Table 8).

$\delta^{13}C$ of grains correlated negatively with GY across the whole set of genotypes and replicates in both planting dates (Fig. 3). Significant correlations using genotypic means were also recorded across the whole set of genotypes as well as within the facultative subset of genotypes in the normal planting and within winter genotypes in the late planting (Table 8). In flag leaves however, the negative correlations of $\delta^{13}C$ against GY were only reported in the late planting across all genotypes as well as within winter genotypes. Nitrogen content of the flag leaf correlated positively with GY across the whole set of genotypes and replicates in both the normal and the

late plantings (Fig. 4A), while nitrogen content in grains correlated negatively with GY (Fig. 4B). However phenotypic correlation (i.e. across the genotype means) between leaf N and GY was only significant at normal planting when both subgroups of genotypes were considered together, while no correlations existed for late planting or within each of the subsets of genotypes (Table 8). N content of kernels correlated negatively with GY across the means of the whole set of genotypes at both the normal and late plantings as well as within the winter subset. Total carbon content and the $\delta^{15}N$ of the flag leaf and grains did not correlate with GY in any case.

Correlations of CT against $\delta^{13}C$ and nitrogen content of the flag leaf and the mature grains were also investigated in both planting dates (Supplemental Table 6). In normal planting and disregarding the placement of the sensor, CT measured at heading related negatively against N of the flag leaf and positively with N content of grains, as well as with the $\delta^{13}C$ of flag leaf and grains. These correlations in the late planting were weaker, though.

Relationships between $\delta^{15}N$ and nitrogen content of the flag leaf against ground and aerial remote sensing (RGB, thermal and multispectral) indices were also displayed (Supplemental Tables 7 and 8). For both $\delta^{15}N$ and N content, correlations were stronger with remote sensing traits measured in normal rather than in late planting, particularly when measured during grain filling.

3.8 Performance of remote sensing techniques and stable isotopes on GY phenotyping

To evaluate the best GY predictors among all remote sensing (RGB, thermal and multispectral) indices and analytical (N content and isotopic parameters) values, multilinear stepwise regression models were tested for both planting dates, and using the genotypic means for GY as well as for all the phenotypic traits evaluated (Table 9). Three different categories of phenotyping models were tested: 1) only including remote sensing indices; 2) only including stable isotope signatures and N content and 3) combining the two previous categories. In general, and for each of these three categories of phenotyping characteristics, models explained better genotypic variability in GY in the normal compared with the late planting within each phenotyping category. Also, models using stable isotopes and nitrogen content alone predicted GY performance more efficiently than these using remote sensing indices alone; nevertheless, the best predictions were attained when both categories of traits were combined (Table 9).

4. Discussion

4.1Effect of planting date and the genotype attitude on wheat performance

Sowing date is regarded as a key factor to adjust wheat growth cycle to the climate conditions prevailing in a site [1]. Late planting is an experimental approach frequently used to evaluate the effect of increased temperature in crop performance [44–46]. The interfering effects of factors other than temperature affecting the growth and development pattern of the crop may be excluded. In our experimental setup, differences in photoperiod were rather minor: one hour (corresponding to 10.39 h and 11.39 h, for the dates for normal and late planting, respectively), from a total annual variation of about 6 h at the latitude of Zamadueñas station). Moreover, both trials were exposed to a pattern of increasing daylength after seedling emergence (considering the days elapsed between sowing and emergence in the normal planting).The current study intended to evaluate the behavior of wheat cultivars planted in different dates in relation with the performance of phenotyping techniques, altogether with the interaction of planting temperature (i.e. planting date) with genotyping characteristics determining flowering induction by low temperature (i.e. winter versus facultative behavior).

Even after removing the effect of phenology (using heading time as a covariate), winter cultivars were still significantly different than facultative cultivars for GY, number of spikes m^{-2}, $\delta^{13}C_{leaf}$ and $\delta^{13}C_{grain}$ and N content of the grain, as well as most of the RGB vegetation indices measured during grain filling. A decrease in GY is expected in the late planting as a result of higher temperatures which, not only shorten the duration of the crop cycle, but also increase respiration

(dark respiration and photorespiration) rates and may eventually expose plants to heat stress during late growth stages [47,48]. Our results suggest that differences in yield between the two genotypic types were (at least in part) established prior grain filling. One factor involved may be the longer phenology (date of heading) of the winter phenotypes which has been reported before [10,49]. Moreover, it has been reported that winter cultivars are more tolerant to low temperature than the facultative ones [7,8]. The negative effect of a late planting on GY was related with a shorter crop duration, which basically caused a decrease in spikes m^{-2}, particularly in the winter genotypes, given their poor flowering. By contrast, facultative cultivars, apart from not having the vernalization requirements to flowering [7,8,50], they express genes that confer heat tolerance [51–53]. The expected rise in temperature associated with climate change [4,5] will make on the long term winter genotypes more vulnerable than facultative ones, highlighting hence the potential adaptive ability of facultative genotypes that can secure better productivity under Mediterranean conditions. The increase in the atmospheric level of CO_2 is not expected to play any differential effect between both categories of genotypes, besides to alleviate the negative effects of heat on the photosynthetic activity.

In the normal planting the $\delta^{13}C$ of both the flag leaf and grains of the winter genotypes were slightly more negative than that of facultative genotypes, indicating better water status experienced by the winter genotypes in spite their somewhat larger crop cycle [54,55]. In agreement with that, days to heading was positively correlated with GY across the whole (winter plus facultative) set of genotypes. By contrast, in the late planting, facultative genotypes exhibited a more negative leaf $\delta^{13}C$ than the winter genotypes, and days to heading were negatively correlated with GY across the whole set of genotypes as well as within winter genotypes. These results indicate that for a late planting, even if under well irrigated conditions shown by the very low $\delta^{13}C$ values of both the flag leaf and the grains (even more negative than for the normal planting), escaping attitude, in terms of reaching fast the reproductive stage, is paramount under Mediterranean conditions as growing temperature increases [55,56].

4.2 RGB and multispectral indices and wheat performance

Among RGB indices, GA, GGA, a* and Hue, altogether with multispectral-derived indices NDVI, EVI, PRI and TCARIOSAVI, are considered as efficient indicators of canopy growth and green vegetation [17]. In the present study, and regardless of data of measurement, these indices correlated in general better with GY in the normal planting compared with the late planting trial. In fact, late planting, by shortening crop cycle, is probably diminishing genotypic differences in canopy biomass and greenness, as well as in ground covering and thus yield. All these aspects may limit the performance of vegetation indices assessing genotypic differences in GY. Different explanations may be argued, as for instance the faster development and shorter crop duration in late planting, which moreover to limiting canopy growth may blur genotypic differences in canopy size as well as in stay green.

Generally, RGB and multispectral vegetation indices correlated better against GY during grain filling than at heading. Comparable results have been reported previously regarding durum wheat [27,41,57], the explanation being these indices, when assessed during grain filling, may catch differences across genotypes in terms of maintaining the photosynthetic capacity of the canopy for longer, which is known as stay green [58]. Besides that, grain filling is at a later stage than heading, and closer to maturity and harvest, therefore more representing the final GY.

Concerning stay green, in the case of CCI, this index reflects the chlorophyll/carotenoid ratio in the canopy, with senescence increasing this ratio. The negative correlation obtained in the late planting, not only across the whole set of genotypes, but also across the winter genotypes, can be explained by the fact the canopy of the winter genotypes remains greener for longer because reproductive stage is delayed (and irregular), and consequently the canopy senescence too. The more the senescence is delayed the poorer the reproductive stage is and consequently GY will be lower. On the contrary in the normal planting, stay green during grain filling is a positive trait in

terms of increasing GY, particularly when water conditions are adequate such in our trials submitted to support irrigation.

Recent reports on barley [26] and maize [17,31] concluded for RGB indices that when assessed from ground they performed as well as assessed aerially. Nevertheless, different factors may explain the poor performance of ground images at heading. For each index differences across the whole set and the subsets of winter and facultative genotypes were similar regardless of being assessed at ground or from an UAV. Nevertheless, the absolute values varied between both ground and aerial acquired indices (Table 4). Ground and aerial measurements were held at the same time (though for ground measures the assessment period was considerably longer than these assessed aerially). Differences in environmental variables possibly affecting the images can be involved. Thus, while measurements during grain filling were performed on a sunny day, measurements during heading took place in a day of alternating sun and clouds. Therefore, sudden and/or transient changes in light conditions may affect the ground measurements. On the other hand, the potential effects of Bidirectional Reflectance Distribution Function (BRDF) were minimized by capturing ground and UAV images at approximately the same time of day and within 2 hours of solar noon. Moreover, at least for the measurements during heading the conditions were partially cloudy which could minimize BRDF effects with diffuse light. The main advantage of ground assessment is that images resolution is higher compared to that of aerial images. In the case of the RGB images, the number of pixels per plot decreases drastically when images are acquired aerially. Nevertheless, aerial images provide full coverage of the entire plots at the same time, while ground assessed RGB images capture only approximately 35% plot area coverage based on ground sample distance calculations (data not shown). In the case of the NDVI measured with the hand spectroradiometer, again only a section of the plot is captured. Besides that, heading is not the optimal period to assess GY differences with RGB indices, particularly given the fact green biomass is larger at this stage than at grain filling. Thus, ground-acquired indices may be more saturated (excess of green because of very dense canopies) and then it is more complicated to assess differences among the genotypes.

4.3 Canopy temperature and wheat performance

Water stress conditions can be detected through measuring CT, where stressed plants reveal higher CT compared to unstressed ones and in fact, negative correlations between CT and GY are expected [59,60]. In our study, even if trials were irrigated, significant negative correlations were found for the normal planting trial from both platforms. Similarly to the vegetation indices, at heading CT measured from the aerial platform correlated stronger against GY than those measured from ground level, whereas similar phenotypic correlations against GY were found during grain filling. In any case the potential advantage of an aerial platform relies in the fact that CT from the entire plots are measured simultaneously, which is not the case when temperature is assessed at ground level in individual plots. Soil but specially environmental conditions (air temperature, wind, sun brightness) may fluctuate from plot to plot throughout the sampling [12]. Moreover, whilst aerial images capture the entire plot canopy, the ground based ones cover only 40% to 50% of each plot's canopy [42].

In our study, a higher CT was coupled not only with a lower yield but also with lower leaf nitrogen content and higher $\delta^{13}C$ values. Comparable relationships have been reported before in wheat under Mediterranean conditions, by combining different water and nitrogen fertilization regimes [27]. The positive correlation of CT with carbon isotopic composition is coherent with the fact a higher $\delta^{13}C$ has been associated with a poorer water status [55]. In the same sense, a poorer water status assessed through high CT, may also negatively affect N accumulation in the plant [27,57,61].

However, CT may be affected by genotype attitude in a way it does not inform on the water status of the crop. The delay in the extrusion of the spikes, together with a larger leaf biomass of the winter genotypes is related with their lower CT during heading and grain filling compared to the facultative ones in both plantings. In fact, leaves transpire more than the non-laminar parts (stems,

ears) of the plant, and therefore the CT is strongly affected by phenology [62]. This should agree with the lower CT observed in the winter compared with facultative subset during grain filling at late panting. Interestingly, for the late planting $\delta^{13}C$ of the flag leaf was higher (less negative) in the winter compared with the facultative group, suggesting poorer water status in the winter cultivars, and no differences in $\delta^{13}C$ of mature grains were found between both groups (winter and facultative). These results in carbon isotope signature further support differences in CT between winter and facultative are not due to differential water status [55] but to phenology (ear emergence).

4.4 Stable isotopes, N content and wheat performance

$\delta^{13}C$ is an efficient and accurate estimator of the effect of water status on stomatal conductance and thus photosynthesis and yield [43,63,64]. Correlations of GY with $\delta^{13}C$ of mature grains were negative and significant in both planting dates, with correlation coefficients usually larger than for remote sensing data against GY. For the late planting $\delta^{13}C$ flag leaf was also negatively correlated with GY. In fact, under Mediterranean field conditions and except for very severe stressed environments, the correlations between $\delta^{13}C$ and GY are negative, which means that genotypes more productive are keeping stomata more open [33,55].

For both the normal and the late planting, the flag leaf of the winter genotypes exhibited higher $\delta^{15}N$ values than the facultative genotypes. While the nitrogen chemical fertilizer used possesses $\delta^{15}N$ values near 0‰, naturally available nitrogen in the soil exhibits values $\delta^{15}N$ clearly higher [65,66]. Therefore, and regardless the planting date, the higher $\delta^{15}N$ values of the winter genotypes may be related with their larger biomass compared with the facultative genotypes, which make the former more demanding of nitrogen sources other than that provided by the chemical fertilizer. In fact, leaf $\delta^{15}N$ was positively related with the RGB (GA, GGA) and multispectral (NDVI, EVI) indices most suited as indicators of green biomass, while it correlated negatively with CT. However, $\delta^{15}N$ did not correlate with GY in any case even if entered as a trait in most of the stepwise models explaining GY.

Nitrogen content of flag leaves in the normal planting was positively correlated with GY, while in mature grains, and for both planting dates, nitrogen content was negatively correlated to GY. In fact, we found a positive correlation between leaf nitrogen against canopy greenness measured as NDVI, GA or GGA measured during grain filling. This agrees with previous results [67] and suggests a higher N content in flag leaves is an indicator for stay-green and thereby for greater yield. Moreover, and for both planting dates, N content in leaves was higher in winter compared with facultative genotypes, which agrees with the delayed phenology of the former in terms of reproductive period. By contrast the negative correlation of nitrogen concentration in grains against GY is just a consequence of a concentration effect related with lower yield [68,69]. In this sense, for the normal panting nitrogen concentration of grains was lower in the winter compared with the facultative genotypes.

4.5 *Phenotyping approaches and grain yield prediction*

Vegetation indices, both multispectral and RGB-derived, proved their efficiency in the normal planting at detecting genotypic variability in GY. Moreover, for late planting even if the stepwise models were less strong than for the normal planting, they still explained a relevant portion of genotypic variability in GY, and again with models using indices assessed at heading working better than those using indices measured at grain filling. These results illustrate the potential advantage of using a combination of selection indices to explain genotypic differences in GY rather than just a single index [17,31]. Furthermore, total nitrogen content and carbon isotopic composition of flag leaves and mature grains proved to be appropriate phenotypical proxies for determining genotypic performance throughout the crop cycle and regardless of the planting date. These traits provide a time-integrated information of the crop performance in terms of water status in the case of $\delta^{13}C$ [55], stay green in case of leaf nitrogen [70] or sink size as for the nitrogen

content in grains [69]. Therefore, these analytical variables, contribute to a better understanding of the physiological differences existing between genotypes attitudes or and their adaptation to different growing conditions. Moreover, by adding these analytical variables the strength of the stepwise models based in remote sensing indices strongly improved regardless of the planting date and stage when remote sensing traits were acquired.

5. Conclusions

This study highlights the importance for wheat phenotyping performance of growing temperature, genotype attitude, trait category, phenological stage when evaluated, and even platform placement. In a normal planting the different remote sensing indices and regardless their nature (RGB or multispectral) performed quite similarly assessing yield. Later evaluation (i.e. at grain filling) performed clearly better than the earlier one (at heading) even if combined (e.g. stepwise) models may palliate such limitation. Concerning placement of the remote sensing sensors (at ground versus aerial) vegetation indices and CT evaluated aerially worked much better than from ground at heading but quite similarly at grain filling. At least on what concerns the RGB cameras potential minor differences between the images captured at the ground level and from the UAV may be due to differences in camera model and sensor (micro 4/3 size LiveMOS Panasonic GX7 vs CMOS Exmor size APS-C Sony QX1 in our study). However, camera comparisons made to the XRite ColorChecker Passport showed correlations r>0.94 for RGB values for both cameras under natural sunlight conditions (data not shown). Therefore, as indicated above other factors like sunlight conditions or the representativeness of the plot area assessed at ground may be involved in the poor performance of ground-acquired indices at heading.

With regard to genotype attitude, no clear pattern emerged; in some cases, remote sensing indices correlated better with GY within winter genotypes and in others the opposite. Late plating conditions strongly decreased the performance of remote sensing approaches for assessing yield. By contrast analytical traits such as $\delta^{13}C$ as well as N content of mature kernels correlated quite similarly against GY regardless planting time and genotype attitude. Taken together these results indicate that for Mediterranean conditions while remote sensing techniques may lose efficiency as phenotyping traits due to miscellaneous factors, analytical traits, such as $\delta^{13}C$ and %N, of kernels are less affected. Moreover, the performance of remote sensing approaches (RGB, multispectral and thermal) aiming to track genotypic differences in grain yield in wheat, can be clearly improved when combined with $\delta^{13}C$ or N of mature kernels. However, the intrinsic limitation of these analytical traits is that they are assessed at maturity, which prevent their use to predict yield before the crop cycle ends. Using hyperspectral remote sensing to improve (in some cases) the ability of single indices to assess traits, or even to use the entire spectrum, in an empirical way, may represent other alternatives. The decreasing cost of hyperspectral imagers, together the improving capacity of data processing may pave the way for adopting these approaches [15].

Acknowledgments

The study was developed within the context of the ERANET Project Concert Japan PCIN-2017-063 and the Project AGL2016-76527-R: from the MINECO, Spanish Government. FR is a recipient of a master thesis grant sponsored by the International Center for Advanced Mediterranean Agronomic Studies (CIHEAM), in collaboration with the Mediterranean Agronomic Institute of Zaragoza (IAMZ) and Lleida University (UdL). JLA acknowledges the support from ICREA Academia, Autonomous Government of Catalonia, Spain.

Author contributions: N.A.G., I.A., M.D.S. and J.L.A. conceived and designed the experiment. N.A. managed and directed the wheat trials at the experimental station of Zamadueñas (Valladolid, Spain). A.G-R., N.A.G. and J.L.A. conducted the field ground measurements.

S.C.K., A.G-R. and F.Z.R carried out the flights for the obtainment of the aerial measurements and processed and analyzed the images. F.Z.R. and M.D.S. run the stable isotope analyses. F.Z.R. did the statistical analysis and wrote the draft paper under the supervision of J.L.A. and M.D.S.

References

[1] J. Hussain, T. Khaliq, A. Ahmad, J. Akhter, S. Asseng, Wheat responses to climate change and its adaptations: a focus on arid and semi-arid environment, Int. J. Environ. Res. 12 (2018) 117–126. doi:10.1007/s41742-018-0074-2.

[2] H. Kahiluoto, J. Kaseva, J. Balek, J.E. Olesen, M. Ruiz-Ramos, A. Gobin, K.C. Kersebaum, J. Takáč, F. Ruget, R. Ferrise, P. Bezak, G. Capellades, C. Dibari, H. Mäkinen, C. Nendel, D. Ventrella, A. Rodríguez, M. Bindi, M. Trnka, Decline in climate resilience of European wheat, Proc. Natl. Acad. Sci. (2018) 1–6. doi:10.1073/pnas.1804387115.

[3] F.X. Oury, C. Godin, A. Mailliard, A. Chassin, O. Gardet, A. Giraud, E. Heumez, J.Y. Morlais, B. Rolland, M. Rousset, M. Trottet, G. Charmet, A study of genetic progress due to selection reveals a negative effect of climate change on bread wheat yield in France, Eur. J. Agron. 40 (2012) 28–38. doi:10.1016/j.eja.2012.02.007.

[4] D.B. Lobell, S.M. Gourdji, The influence of climate change on global crop productivity, Plant Physiol. 160 (2012) 1686–1697. doi:10.1104/pp.112.208298.

[5] D.B. Lobell, W. Schlenker, J. Costa-Roberts, Climate trends and global crop production since 1980, Science. 333 (2011) 616–620. doi:10.1126/science.1204531.

[6] G.O. Ferrara, M.G. Mosaad, V. Mahalakshmi, S. Rajaram, Photoperiod and vernalisation response of mediterranean wheats, and implications for adaptation, Euphytica. 100 (1998) 377–384. doi:10.1023/A:1018375616915.

[7] B. Trevaskis, D.J. Bagnall, M.H. Ellis, W.J. Peacock, E.S. Dennis, MADS box genes control vernalization-induced flowering in cereals, Proc. Natl. Acad. Sci. 100 (2003) 13099–13104. doi:10.1073/pnas.1635053100.

[8] U. Steinfort, B. Trevaskis, S. Fukai, K.L. Bell, M.F. Dreccer, Vernalisation and photoperiod sensitivity in wheat: impact on canopy development and yield components, F. Crop. Res. 201 (2017) 108–121. doi:10.1016/j.fcr.2016.10.012.

[9] K. Al-Khatib, G.M. Paulsen, Mode of high temperature injury to wheat during grain development, Physiol. Plant. 61 (1984) 363–368. doi:10.1111/j.1399-3054.1984.tb06341.

[10] B. Wang, D.L. Liu, S. Asseng, I. Macadam, Q. Yu, Impact of climate change on wheat flowering time in eastern Australia, Agric. For. Meteorol. 209–210 (2015) 11–21. doi:10.1016/j.agrformet.2015.04.028.

[11] M.P. Reynolds, M. Balota, M.I.B. Delgado, I. Amani, R.A. Fischer, Physiological and morphological traits associated with spring wheat yield under hot, irrigated conditions, Aust. J. Plant Physiol. 21 (1994) 717–730. doi:10.1071/PP9940717.

[12] J.L. Araus, J.E. Cairns, Field high-throughput phenotyping: the new crop breeding frontier, Trends Plant Sci. 19 (2014) 52–61. doi:10.1016/j.tplants.2013.09.008.

[13] S. Sankaran, L.R. Khot, C.Z. Espinoza, S. Jarolmasjed, V.R. Sathuvalli, G.J. Vandemark, P.N. Miklas, A.H. Carter, M.O. Pumphrey, N.R. Knowles, M.J. Pavek, Low-altitude , high-resolution aerial imaging systems for row and field crop phenotyping : a review, Eur. J. Agron. 70 (2015) 112–123. doi:10.1016/j.eja.2015.07.004.

[14] V.S. Weber, J.L. Araus, J.E. Cairns, C. Sanchez, A.E. Melchinger, E. Orsini, Prediction of grain yield using reflectance spectra of canopy and leaves in maize plants grown under different water regimes, F. Crop. Res. 128 (2012) 82–90. doi:10.1016/j.fcr.2011.12.016.

[15] J.L. Araus, S.C. Kefauver, M. Zaman-Allah, M.S. Olsen, J.E. Cairns, Translating high-throughput phenotyping into genetic gain, Trends Plant Sci. 23 (2018) 451–466. doi:10.1016/j.tplants.2018.02.001.

[16] A.S. Ray, Remote sensing in agriculture, Int. J. Environ. Agric. Biotechnol. 1 (2016) 2456–1878. doi:10.22161/ijeab/1.3.8.

[17] A. Gracia-Romero, O. Vergara-Díaz, C. Thierfelder, J.E. Cairns, S.C. Kefauver, J.L. Araus, Phenotyping conservation agriculture management effects on ground and aerial remote sensing assessments of maize hybrids performance in zimbabwe, Remote Sens. 10 (2018) 1–21. doi:10.3390/rs10020349.

[18] S.C. Kefauver, R. Vicente, O. Vergara-Díaz, J.A. Fernandez-Gallego, S. Kerfal, A. Lopez, J.P.E. Melichar, M.D. Serret Molins, J.L. Araus, Comparative UAV and field phenotyping to assess yield and nitrogen use efficiency in hybrid and conventional barley, Front. Plant Sci. 8 (2017) 1–15. doi:10.3389/fpls.2017.01733.

[19] G. Asrar, M. Fuchs, E.T. Kanemasu, J.L. Hatfield, Estimating absorbed photosynthetic radiation and leaf area index from spectral reflectance in wheat, Agron. J. 76 (1984) 300–306. doi:10.2134/agronj1984.00021962007600020029x.

[20] A.L. Nguy-Robertson, Y. Peng, A.A. Gitelson, T.J. Arkebauer, A. Pimstein, I. Herrmann, A. Karnieli, D.C. Rundquist, D.J. Bonfil, Agricultural and forest meteorology estimating green LAI in four crops : potential of determining optimal spectral bands for a universal algorithm, Agric. For. Meteorol. 192–193 (2014) 140–148. doi:10.1016/j.agrformet.2014.03.004.

[21] J.A. Gamon, K.F. Huemmrich, C.Y.. S. Wong, I. Ensminger, S. Garrity, D.Y. Hollinger, A. Noormets, J. Peñuelas, A remotely sensed pigment index reveals photosynthetic phenology in evergreen conifers., Proc. Natl. Acad. Sci. U. S. A. 113 (2016) 13087–13092.

[22] A.A. Gitelson, A. Viña, V. Ciganda, D.C. Rundquist, T.J. Arkebauer, Remote estimation of canopy chlorophyll content in crops, Geophys. Res. Lett. 32 (2005) 1–4. doi:10.1029/2005GL022688.

[23] D. Haboudane, N. Tremblay, J.R. Miller, P. Vigneault, Remote estimation of crop chlorophyll content using spectral indices derived from hyperspectral data, IEEE Trans. Geosci. Remote Sens. 46 (2008) 423–436. doi:10.1109/TGRS.2007.904836.

[24] I. Herrmann, A. Karnieli, D.J. Bonfil, Y. Cohen, V. Alchanatis, SWIR-based spectral indices for assessing nitrogen content in potato fields, Int. J. Re. 31 (2010) 5127–5143. doi:10.1080/01431160903283892.

[25] W. Feng, X. Yao, Y. Zhu, Y.C. Tian, W.X. Cao, Monitoring leaf nitrogen status with hyperspectral reflectance in wheat, Eur. J. Agron. 28 (2008) 394–404. doi:10.1016/j.eja.2007.11.005.

[26] J.M. Costa, O.M. Grant, M.M. Chaves, Thermography to explore plant-environment interactions, J. Exp. Bot. 64 (2013) 3937–3949. doi:10.1093/jxb/ert029.

[27] S. Yousfi, N. Kellas, L. Saidi, Z. Benlakehal, L. Chaou, D. Siad, F. Herda, M. Karrou, O. Vergara, A. Gracia, J.L. Araus, M.D. Serret, Comparative performance of remote sensing methods in assessing wheat performance under mediterranean conditions, Agric. Water Manag. 164 (2016) 137–147. doi:10.1016/j.agwat.2015.09.016.

[28] M.S. Moran, T.R. Clarke, Y. Inoue, A. Vidal, Estimating crop water deficit using the relation between surface-air temperature and spectral vegetation index, Remote Sens. Environ. 49 (1994) 246–263. doi:10.1016/0034-4257(94)90020-5.

[29] R.D. Jackson, R.J. Reginato, S.B. Idso, Wheat canopy temperature: a practical tool for evaluating water requirements, Water Resour. Res. 13 (1988) 651–656. doi:10.1029/WR013i003p0065.

[30] J. Casadesús, D. Villegas, Conventional digital cameras as a tool for assessing leaf area index and biomass for cereal breeding, J. Integr. Plant Biol. 56 (2014) 7–14. doi:10.1111/jipb.12117.

[31] A. Gracia-Romero, S.C. Kefauver, O. Vergara-Díaz, M.A. Zaman-Allah, B.M. Prasanna, J.E. Cairns, J.L. Araus, Comparative performance of ground vs. aerially assessed RGB and multispectral indices for early-growth evaluation of maize performance under phosphorus fertilization, Front. Plant Sci. 8 (2017) 1–13. doi:10.3389/fpls.2017.02004.

[32] J.L. Araus, L. Cabrera-Bosquet, M.D. Serret, J. Bort, M.T. Nieto-Taladriz, Combined use of $\delta^{13}C$, $\delta^{18}O$ and $\delta^{15}N$ tracks nitrogen metabolism and genotypic adaptation of durum wheat to salinity and water deficit, Funct. Plant Physiol. 40 (2013) 595–608. doi:10.1071/FP12254.

[33] R. Sanchez-Bragado, G. Molero, M.P. Reynolds, J.L. Araus, Relative contribution of shoot and ear photosynthesis to grain filling in wheat under good agronomical conditions assessed by differential organ $\delta^{13}C$, J. Exp. Bot. 65 (2014) 5401–5413. doi:10.1093/jxb/eru298.

[34] R. Sanchez-Bragado, G. Molero, M.P. Reynolds, J.L. Araus, Photosynthetic contribution of the ear to grain filling in wheat: a comparison of different methodologies for evaluation, J. Exp. Bot. 67 (2016) 2787–2798. doi:10.1093/jxb/erw116.

[35] M.J. Santos, E.L. Hestir, S. Khanna, S.L. Ustin, Image spectroscopy and stable isotopes elucidate functional dissimilarity between native and nonnative plant species in the aquatic environment, New Phytol. 193 (2012) 683–695. doi:10.1111/j.1469-8137.2011.03955.x.

[36] A. Singh, S.P. Serbin, B.E. McNeil, C.C. Kingdon, P.A. Townsend, Imaging spectroscopy algorithms for mapping canopy foliar chemical and morphological traits and their uncertainties, Ecol. Appl. 25 (2015) 2180–2197. doi:10.1890/14-2098.1.

[37] J. Crain, I. Ortiz-Monasterio, B. Raun, Evaluation of a reduced cost active NDVI sensor for crop nutrient management, J. Sensors. 2012 (2012) 10. doi:10.1155/2012/582028.

[38] G. Barmeier, U. Schmidhalter, High-throughput phenotyping of wheat and barley plants grown in single or few rows in small plots using active and passive spectral proximal sensing, SENSORS. 16 (2016) 1–14. doi:10.3390/s16111860.

[39] J. Bendig, A. Bolten, S. Bennertz, J. Broscheit, S. Eichfuss, G. Bareth, Estimating biomass of barley using crop surface models (CSMs) derived from UAV-based RGB imaging, Remote Sens. 6 (2014) 10395–10412. doi:10.3390/rs61110395.

[40] A. Gracia-Romero, S.C. Kefauver, J.A. Fernandez-Gallego, O. Vergara-Díaz, J.L. Araus, UAV and ground image-based phenotyping : a proof of concept with durum wheat, Remote Sens. 11 (2019) 1–25. doi:10.3390/rs11101244.

[41] J. Casadesùs, Y. Kaya, J. Bort, M.M. Nachit, J.L. Araus, S. Amor, G. Ferrazzano, F. Maalouf, M. Maccaferri, V. Martos, H. Ouabbou, D. Villegas, Using vegetation indices derived from conventional digital cameras as selection criteria for wheat breeding in water-limited environments, Ann. Appl. Biol. 150 (2007) 227–236. doi:10.1111/j.1744-7348.2007.00116.x.

[42] M.L. Buchaillot, A. Gracia-Romero, O. Vergara-Diaz, M.A. Zaman-Allah, A. Tarekegne, J.E. Cairns, B.M. Prasanna, J.L. Araus, S.C. Kefauver, Evaluating maize genotype performance under low nitrogen conditions using RGB UAV phenotyping techniques, Sensors. 19 (2019) 1–27. doi:10.3390/s19081815.

[43] G.D. Farquhar, J.R. Ehleringer, K.T. Hubick, Carbon isotope discrimination and photosynthesis, Annu. Rev. Plant Physiol. 40 (1989) 503–537. doi:10.1146/annurev.pp.40.060189.002443.

[44] R.K. Jat, P. Singh, M.L. Jat, M. Dia, H.S. Sidhu, S.L. Jat, D. Bijarniya, H.S. Jat, C.M. Parihar, U. Kumar, S.L. Ridaura, Heat stress and yield stability of wheat genotypes under different sowing dates across agro-ecosystems in India, F. Crop. Res. 218 (2018) 33–50. doi:10.1016/j.fcr.2017.12.020.

[45] P. Paymard, M. Bannayan, R.S. Haghighi, Analysis of the climate change effect on wheat production systems and investigate the potential of management strategies, Nat. Hazards. 91 (2018) 1237–1255. doi:10.1007/s11069-018-3180-8.

[46] W.J. Sacks, D. Deryng, J.A. Foley, N. Ramankutty, Crop planting dates: an analysis of global patterns, Glob. Ecol. Biogeogr. 19 (2010) 607–620. doi:10.1111/j.1466-8238.2010.00551.x.

[47] I. Elbasyoni, Performance and stability of commercial wheat cultivars under terminal heat stress, Agronomy. 8 (2018) 1–20. doi:10.3390/agronomy8040037.

[48] M.P. Reynolds, R.P. Singh, A. Ibrahim, O.A.A. Ageeb, A. Larque-Saavedra, J.S. Quick, Evaluating physiological traits to complement empirical selection for wheat in warm environments, Euphytica. 100 (1998) 85–94. doi:10.1023/A:1018355906553.

[49] B.I. Cook, E.M. Wolkovich, C. Parmesan, Divergent responses to spring and winter warming drive community level flowering trends, PNAS. 109 (2012) 1–6. doi:10.1073/pnas.1118364109.

[50] H.M. Rawson, M. Zajac, L.D.J. Penrose, Effect of seedling temperature and its duration on development of wheat cultivars differing in vernalization response, F. Crop. Res. 57 (1998) 289–300. doi:10.1016/S0378-4290(98)00073-2.

[51] B. Trevaskis, M.N. Hemming, E.S. Dennis, W.J. Peacock, The molecular basis of vernalization-induced flowering in cereals, Trends Plant Sci. 12 (2007) 352–357. doi:10.1016/j.tplants.2007.06.010.

[52] A.A. Khan, M.R. Kabir, Evaluation of spring wheat genotypes (*Triticum aestivum* L.) for heat stress tolerance using different stress tolerance indices, Cercet. Agron. Mold. 47 (2015) 49–63. doi:10.1515/cerce-2015-0004.

[53] M.S. Lopes, I. El-Basyoni, P.S. Baenziger, S. Singh, C. Royo, K. Ozbek, H. Aktas, E. Ozer, F. Ozdemir, A. Manickavelu, T. Ban, P. Vikram, Exploiting genetic diversity from landraces in wheat breeding for adaptation to climate change, J. Exp. Bot. 66 (2015) 3477–3486. doi:10.1093/jxb/erv122.

[54] W.R. Whalley, C.W. Watts, A.S. Gregory, S.J. Mooney, L.J. Clark, A.P. Whitmore, The effect of soil strength on the yield of wheat, Plant Soil. 306 (2008) 237–247. doi:10.1007/s11104-008-9577-5.

[55] J.L. Araus, D. Villegas, N. Aparicio, L.F. Garcıa del Moral, S. El-Hani, Y. Rharrabti, J.P. Ferrio, C. Royo, Environmental factors determining carbon isotope discrimination and yield in durum wheat under mediterranean conditions, Crop Sci. 43 (2003) 170–180. doi:10.2135/cropsci2003.0170.

[56] S.P. Loss, K.H.M. Siddique, Orphological and physiological traits associated with wheat yield increases in mediterranean environments, Adv. Agron. 52 (1994) 229–276.

[57] A. Elazab, J. Bort, B. Zhou, M.D. Serret, M.T. Nieto-Taladriz, J.L. Araus, The combined use of vegetation indices and stable isotopes to predict durum wheat grain yield under contrasting water conditions, Agric. Water Manag. 158 (2015) 196–208. doi:10.1016/j.agwat.2015.05.003.

[58] G.J. Rebetzke, J.A. Jimenez-Berni, W.D. Bovill, D.M. Deery, R.A. James, High-throughput phenotyping technologies allow accurate selection of stay-green, J. Exp. Bot. 67 (2016) 4919–4924. doi:10.1093/jxb/erw304.

[59] M.A. Joshi, S. Faridullah, A. Kumar, Effect of heat stress on crop phenology, yield and seed quality attributes of wheat (triticum aestivum L.), J. Agrometeorol. 18 (2016) 206–215. https://search-proquest-com.sire.ub.edu/docview/1868569813?accountid=15293%0A.

[60] S. Thapa, K.E. Jessup, G.P. Pradhan, J.C. Rudd, S. Liu, J.R. Mahan, R.N. Devkota, J.A. Baker, Q. Xue, Canopy temperature depression at grain filling correlates to winter wheat yield in the U.S. southern high plains, F. Crop. Res. 217 (2018) 11–19. doi:10.1016/j.fcr.2017.12.005.

[61] S. Yousfi, M.D. Serret, J.L. Araus, Shoot $\delta^{15}N$ gives a better indication than ion concentration or $\delta^{13}C$ of genotypic differences in the response of durum wheat to salinity, Funct. Plant Biol. 36 (2009) 144–155. doi:10.1111/pce.12055.

[62] B. Zhou, A. Elazab, J. Bort, A. Sanz-Sáez, M.T. Nieto-Taladriz, M.D. Serret, J.L. Araus, Agronomic and physiological responses of chinese facultative wheat genotypes to high-yielding mediterranean conditions, J. Agric. Sci. 154 (2016) 870–889. doi:10.1017/S0021859615000817.

[63] T. Ahmad Yasir, D. Min, X. Chen, A. Gerard, Y. Hu, The association of carbon isotope discrimination (Δ) with gas exchange parameters and yield traits in chinese bread wheat cultivars under two water regimes, Agric. Water Manag. 119 (2013) 111–120. doi:10.1016/j.agwat.2012.11.020.

[64] G.D. Farquhar, R.A. Richards, Isotopic composition of plant carbon correlates with water-use efficiency of wheat genotypes, Aust. J. Plant Physiol. 11 (1984) 539–552. doi:10.1071/PP9840539.

[65] L.I. Wassenaar, Evaluation of the origin and fate of nitrate in the abbotsford aquifer using the isotopes of $\delta^{15}N$ and $\delta^{18}O$ in NO_3^-, Appl. Geochemistry. 10 (1995) 391–405. doi:10.1016/0883-2927(95)00013-a.

[66] S.J. Kerley, S.C. Jarvis, Preliminary studies of the impact of excreted N on cycling and uptake of N in pasture systems using natural abundance stable isotopic discrimination, Plant Soil. 178 (1996) 287–294. doi:10.1007/BF00011595.

[67] J.L. Araus, T. Amaro, Y. Zuhair, M.M. Nachit, Effect of leaf structure and water status on carbon isotope discrimination in field-grown durum wheat, Plant, Cell Environ. 20 (1997) 1484–1494. doi:10.1046/j.1365-3040.1997.d01-43.x.

[68] Z. Chamekh, C. Karmous, S. Ayadi, A. Sahli, M. Belhaj Fraj, S. Yousfi, S. Rezgui, N. Ben Aissa, M.D. Serret, I. McCann, Y. Trifa, H. Amara, J.L. Araus, Comparative performance of $\delta^{13}C$, ion accumulation and agronomic parameters for phenotyping durum wheat genotypes under various irrigation water salinities, Ann. Appl. Biol. 170 (2017) 229–239.

[69] J.L. Araus, T. Amaro, J. Casadesús, A. Asbati, M.M. Nachit, Relationships between ash content, carbon isotope discrimination and yield in durum wheat, Aust. J. Plant Physiol. 25 (1998) 835–842. doi:10.1071/PP98071.

[70] M.S. Lopes, M.P. Reynolds, Stay-green in spring wheat can be determined by spectral reflectance measurements (normalized difference vegetation index) independently from phenology, J. Exp. Bot. 63 (2012) 3789–3798. doi:10.1093/jxb/ers071.

[71] A. Huete, K. Didan, H. Miura, E.P. Rodriguez, X. Gao, L.F. Ferreira, Overview of the radiometric and biopyhsical performance of the MODIS vegetation indices, Remote Sens. Environ. 83 (2002) 195–213. doi:10.1016/S0034-4257(02)00096-2.

[72] G. Rondeaux, M. Steven, F. Baret, Optimization of soil-adjusted vegetation indices, Remote Sens. Environ. 55 (1996) 95–107. doi:10.1016/0034-4257(95)00186-7.

[73] J.A. Gamon, L. Serrano, J.S. Surfus, The photochemical reflectance index: an optical indicator of photosynthetic radiation use efficiency across species, functional types, and nutrient levels, Oecologia. 112 (1997) 492–501.

[74] D. Haboudane, J.R. Miller, N. Tremblay, P.J. Zarco-Tejada, L. Dextraze, Integrated narrow-band vegetation indices for prediction of crop chlorophyll content for application to precision agriculture, Remote Sens. Environ. 81 (2002) 416–426. doi:10.1016/S0034-4257(02)00018-4.

[75] J.A. Gamon, L. Serrano, J.S. Surfus, The photochemical reflectance index: an optical indicator of photosynthetic radiation use efficiency across species, functional types, and nutrient levels, Oecologia. 112 (1997) 492–501. doi:10.1007/s004420050337.

[76] C. Zhang, I. Filella, D. Liu, R. Ogaya, J. Llusià, D. Asensio, J. Peñuelas, Photochemical reflectance index (PRI) for detecting responses of diurnal and seasonal photosynthetic activity to experimental drought and warming in a mediterranean shrubland, Remote Sens. 9 (2017) 1–21. doi:10.3390/rs9111189.

[77] M.F. Garbulsky, J. Peñuelas, J. Gamon, Y. Inoue, I. Filella, The photochemical reflectance index (PRI) and the remote sensing of leaf, canopy and ecosystem radiation use efficiencies. a review and meta-analysis, Remote Sens. Environ. 115 (2011) 281–297. doi:10.1016/j.rse.2010.08.023.

Figure legends:

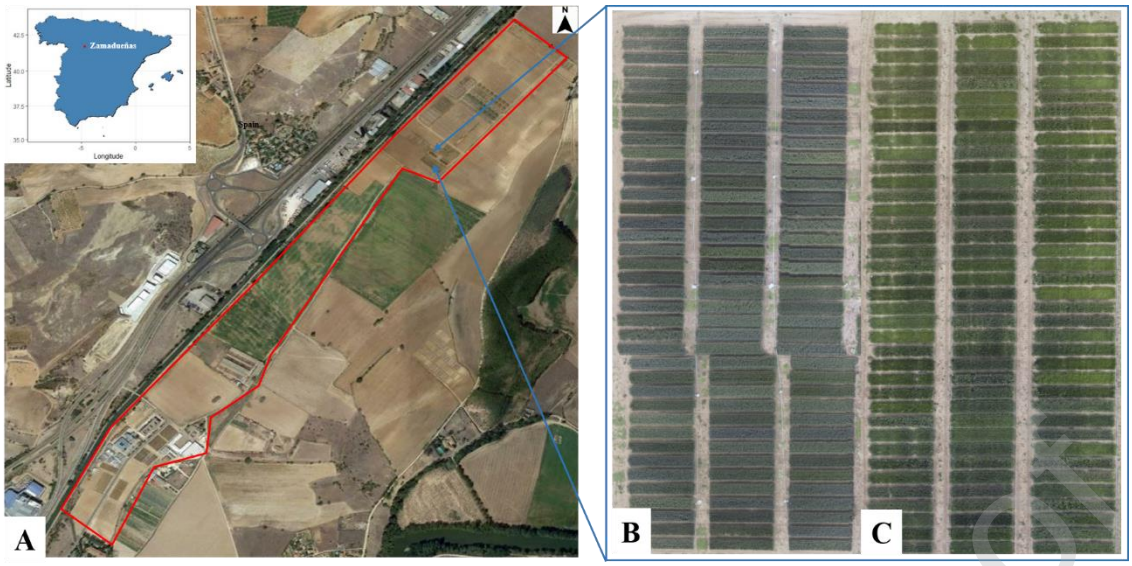

Fig. 1: Map of the location (red point) and the satellite image of the experimental station of Zamadueñas (ITACyL), Valladolid, Spain (A). RGB ortho-mosaics of the normal planting (B) and the late planting (C) trials during late heading. The shift in plot placement of normal planting was due to a problem during planting.

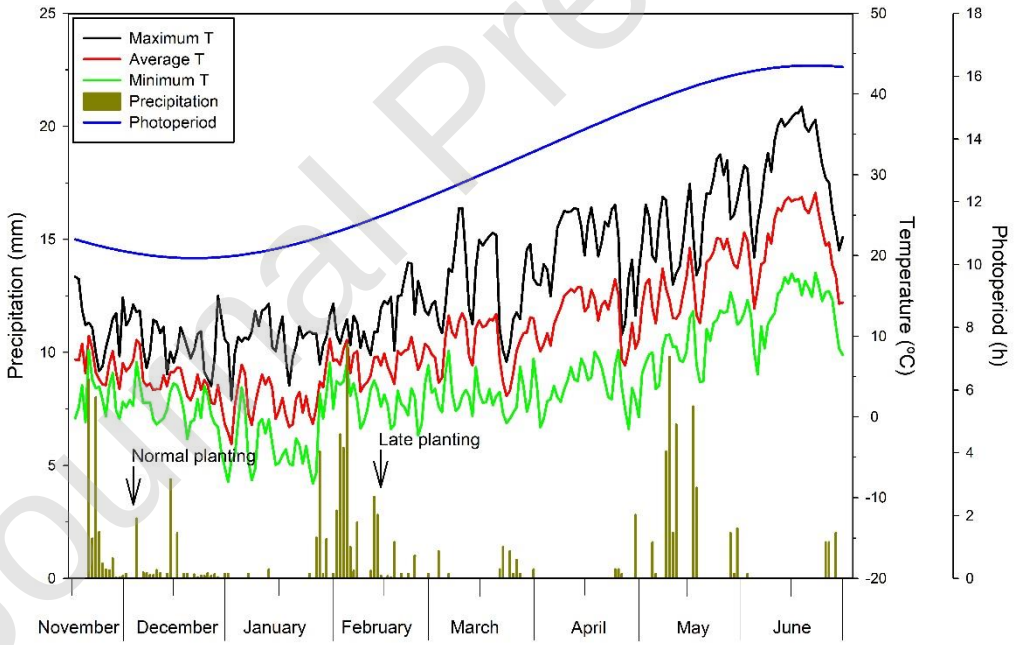

Fig. 2: Weekly precipitation, temperature (average, minimum and maximum) and photoperiod during the growing period covering both planting trials.

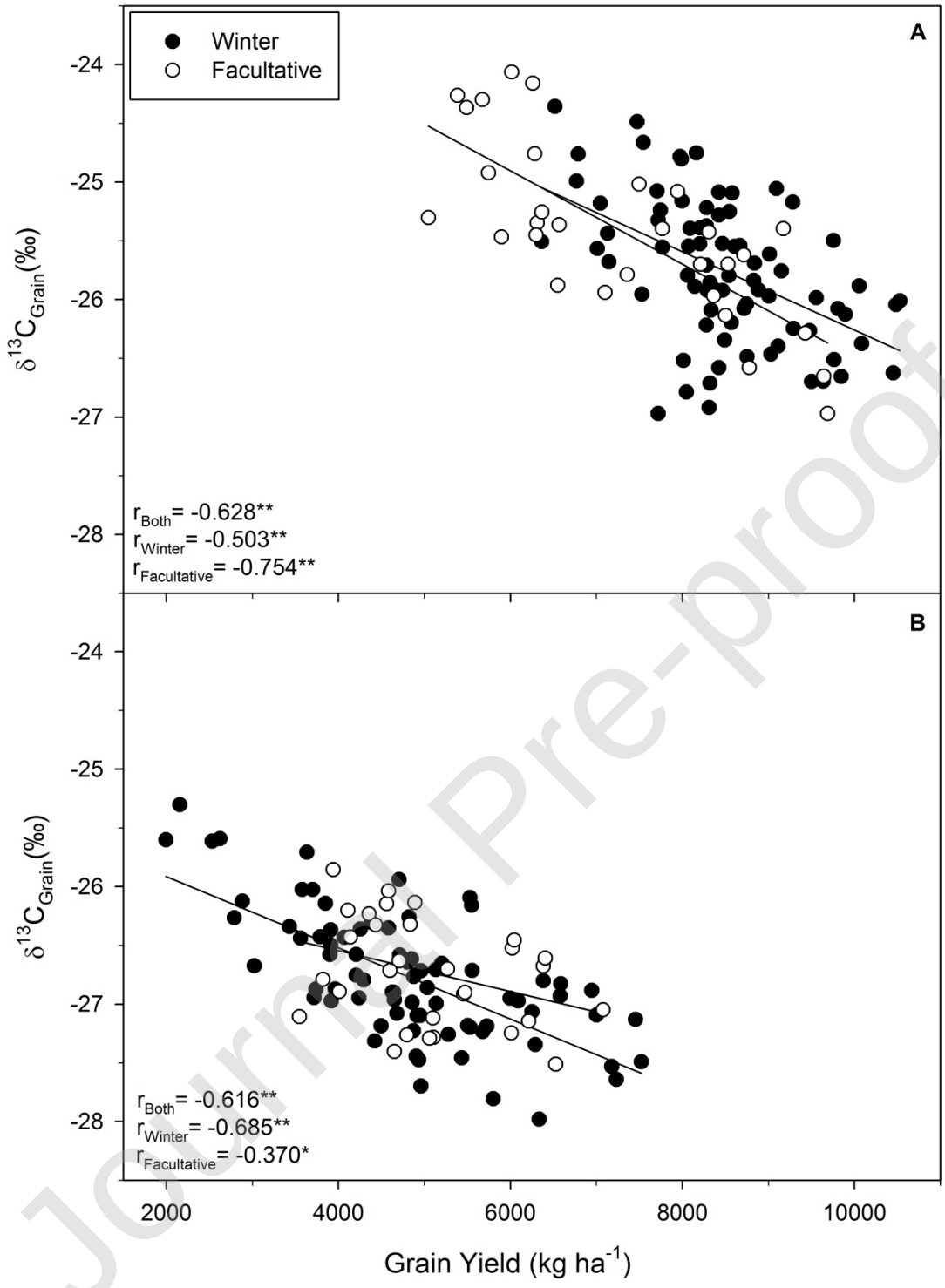

Fig. 3: Relationship between grain yield (GY) and carbon isotope composition ($\delta^{13}C$) of mature grains, sorted by wheat genotype attitude (winter vs facultative), in both normal planting date (A) and late planting date (B). Each point represents a replication (i.e. plot value) for a given cultivar and growing condition.

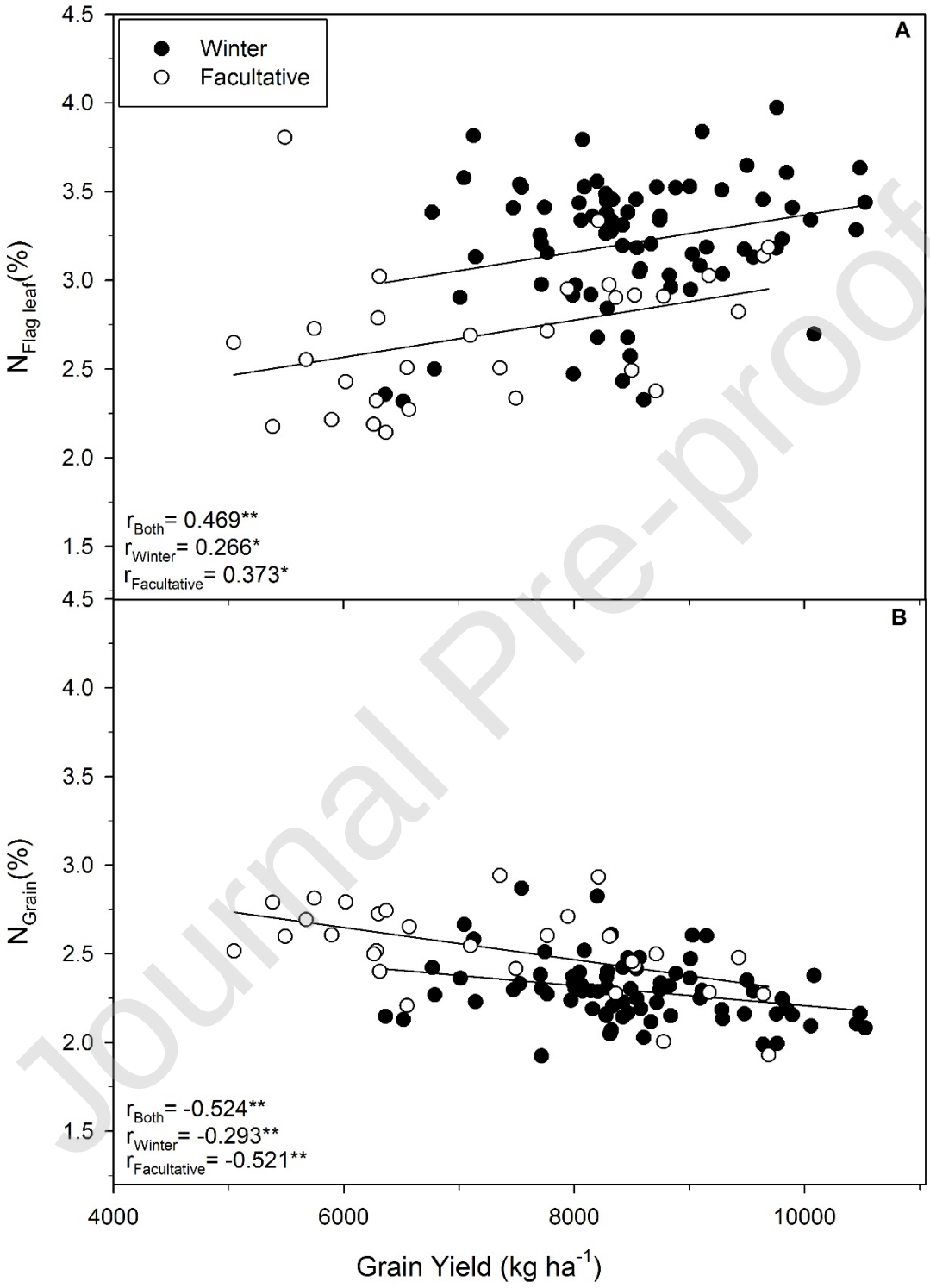

Fig. 4: Relationship between grain yield (GY) and nitrogen content (N) of flag leaves (A) and mature grains (B), sorted by genotypes attitude (winter vs facultative) in normal planting date. Each point represents a replication (i.e. plot value) for a given cultivar and growing condition.

Table 1: List of the 38 wheat varieties used in the study, with their provenance, register number and sorted by their attitude (winter and facultative): 36 were bread wheats (*Triticum aestivum* L), while the other two were durum wheats (*Triticum turgidum* L. ssp. *Durum* (Desf.) Husn.). For each cultivar the register number is specific to the country where the cultivar was registered. Information can be accessed through the variety finder web of the Community Plant Variety Office (CPVO): https://cpvo.europa.eu/en/cpvo-variety-finder

Genotype	Nature	Attitude	Provenance (seed company)	Spanish register number	Genotype	Nature	Attitude	Provenance (seed company)	Spanish register number
ATOMO	*bread*	Facultative	LG SEEDS	20090316	**REBELDE**	*bread*	Winter	BATLLE	20132043
BISANZIO	*bread*	Facultative	AGRAR	20151856	**RIMBAUD**	*bread*	Winter	BATLLE	1023863-
CREDIT	*durum*	Facultative	PRO.SE.ME	20101512	**TRIBAT**	*bread*	Winter	BATLLE	20120245
GALERA	*bread*	Facultative	LG SEEDS	20001714	**CHAMBO**	*bread*	Winter	LG SEEDS	20110170
TOGANO	*bread*	Facultative	ROLLY	20042601	**COMPLICE**	*bread*	Winter	MARISA	20160212
VALBONA	*bread*	Facultative	PRO.SE.ME	20061701	**COSMIC**	*bread*	Winter	AGRUSA	4048820
MIMMO	*durum*	Facultative	PRO.SE.ME	20101513	**IPPON**	*bread*	Winter	FLORIMON DESPREZ	20151563
ENEAS	*bread*	Facultative	DAFISA	20090257	**NEMO**	*bread*	Winter	AGRUSA	20143383
08THES1262	*bread*	Facultative	BATLLE	20114988	**OREGRAIN**	*bread*	Winter	FLORIMON DESPREZ	20120181
ARTHUNICK	*bread*	Facultative	LG SEEDS	20021627	**PR22R58**	*bread*	Winter	PROVASE	20041719
ALHAMBRA	*bread*	Facultative	LG SEEDS	20122397	**SOBERBIO**	*bread*	Winter	CAUSSADE	20151744
ALBERTUS	*bread*	Winter	PRO.SE.ME	20130238	**SOISSON**	*bread*	Winter	AGRUSA	199850256
ALGORITMO	*bread*	Winter	RGT	20160437	**MH1307**	*bread*	Winter	KWS	Advanced breeding line
BOLOGNA	*bread*	Winter	BATLLE	20152157	**MH1341**	*bread*	Winter	KWS	Advanced breeding line
DOLLY	*bread*	Winter	ROLLY	20101741	**MH1411**	*bread*	Winter	KWS	Advanced breeding line
FORCALLI	*bread*	Winter	KWS	1006401	**MH1444**	*bread*	Winter	KWS	Advanced breeding line
INGENIO	*bread*	Winter	AGRUSA	20062285	**CRACKLIN**	*bread*	Winter	LG SEEDS	19990012
GHAYTA	*bread*	Winter	AGRUSA	20122320	**MARCOPOLO**	*bread*	Winter	RGT	20132034
MECANO	*bread*	Winter	AGRUSA	20100121	**SEPTIMA**	*bread*	Winter	AGRAR	20093-

Table 2: Indices derived from RGB and multispectral visible and near infrared bands.

Function	Index	Equation	Reference
Greenness	Green Area (GA)	60^o <Hue< 180^o	[41]
	Greener Area (GGA)	80^o <Hue< 180^o	[41]
	Enhanced Vegetation Index (EVI)	$2.5 \times ((R_{NIR} - R_{Red}) / (R_{NIR} + 6 \times R_{Red} - 7.5 \times R_B + 1))$	[71]
	Normalized Difference Vegetation Index (NDVI)	$(R_{NIR} - R_{Red}) / (R_{NIR} + R_{Red})$	[58]
	Optimized Soil-Adjusted Vegetation Index (OSAVI)	$(R_{780} - R_{670}) / (R_{780}+R_{670}+0.16)$	[72]
Photosynthetic Activity	Photochemical Reflectance Index (PRI)*	$(R_{550} - R_{570}) / (R_{550} + R_{570})$	[73]
	Chlorophyll/Carotenoid index (CCI)	$(R_{550} - R_{670}) / (R_{550} + R_{670})$	[21]
Leaf pigments	Transformed Chlorophyll Absorption Index (TCARI)	$3 \times (R_{700} - R_{670}) - 0.2 \times (R_{700} - R_{550}) \times (R_{700x} / R_{670})$	[74]
	Index Ratio (TCARIOSAVI)	TCARI / OSAVI	[74]

** For the PRI index, R_{550} is used instead of the R_{531} proposed by Gamon et al.* [75]*, given the limitation in specific wavelengths of the multispectral camera used* [76,77]

Table 3: Effect of planting date and genotype attitude on wheat grain yield (kg ha^{-1}), days to heading, grain dry weigh per spike, number of grains per spike, thousand grain weigh (TGW), and number of spikes per area. Range of genotypic values within each category (winter versus facultative) of cultivars are shown in parenthesis.

	Yield (kg ha^{-1})	**Genotypic Yield (kg ha^{-1})**	**Days to heading**	**Grain weight spike^{-1} (g)**	**Grains spike^{-1}**	**TGW (g)**	**Nº spikes m^{-2}**
Normal planting							
All	8161±115	(5694-9893)	149±1	1.75±0.03	43.11±0.62	40.90±0.58	607±10
Winter	8498^{a}±104	(7344-9893)	152^{a}±1	1.71^{b}±0.03	43.96^{a}±0.69	39.01^{b}±0.55	622^{a}±11
Facultative	7296^{b}±251	(5694-9212)	143^{b}±1	1.90^{a}±0.1	40.94 ^{b}±1.22	45.76^{a}±1.06	568 ^{b}±22
Late planting							
All	4894±110	(2770-5961)	104±2	-	-	-	476±10
Winter	4806^{a}±142	(2770-5961)	109^{a}±1	-	-	-	482^{a}±12
Facultative	5095^{a}±156	(4330-5907)	90^{b}±1	-	-	-	461^{a}±18
ANOVA							
PD	<0.001	-	<0.001	-	-	-	<0.001
A	<0.05	-	<0.001	-	-	-	<0.05
PD x A	<0.001	-	<0.001	-	-	-	0.617

Values are means ± standard error of the whole set (38) of genotypes and the winter (27) and facultative (11) subsets of genotypes. Levels of signification for the ANOVA: P<0.01 and P<0.001. PD, Planting date; A, Attitude. Within each planting date, means exhibiting different letters are significantly different (P < 0.05) by t-student on independent samples.

Table 4: Effect of wheat planting dates (normal vs late), and placement of the sensors (aerial vs ground) on RGB and multispectral indices assessed in different phenological stages (Heading vs grain filling).

		RGB Indices										
		Hue.g	a*.g	b*.g	GA.g	GGA.g	Hue.a	a*.a	b*.a	GA.a	GGA.a	NDVI.g
Heading	*Normal planting*											
	All	108±1	-12.6±0.3	15.2±0.3	0.88±0.01	0.75±0.01	140±3	-7.1±0.1	7.7±0.3	0.76±0.02	0.74±0.02	0.71±0.01
	Winter	107^{a}±1	-12.5^{a}±0.3	15.2^{a}±0.4	0.88^{a}±0.01	0.75^{a}±0.01	145^{a}±3	-6.9^{a}±0.1	7.1^{b}±0.3	0.73^{b}±0.02	0.71^{b}±0.02	0.71^{a}±0.01
	Facultative	110^{a}±1	-13.1^{a}±0.5	15.1^{a}±0.4	0.88^{a}±0.01	0.75^{a}±0.02	127^{b}±4	-7.7^{b}±0.2	9.1^{a}±0.5	0.83^{a}±0.02	0.81^{a}±0.02	0.71^{a}±0.01
	Late planting											
	All	-	-	-	-	-	93±2	-10.1±0.2	16.4±0.5	0.95±0.01	0.72±0.03	0.76±0.01
	Winter	-	-	-	-	-	93^{a}±2	-10.4^{b}±0.2	16.9^{a}±0.7	0.95^{a}±0.01	0.73^{a}±0.03	0.77^{a}±0.01
	Facultative	-	-	-	-	-	912^{a}±2	-9.4^{a}±0.2	15.3^{a}±0.7	0.95^{a}±0.01	0.71^{a}±0.05	0.72^{b}±0.01
	ANOVA											
	PD	-	-	-	-	-	<0.001	<0.001	<0.001	<0.001	<0.001	<0.001
	A	-	-	-	-	-	0.026	0.238	0.702	0.024	0.392	<0.001
	PD x A	-	-	-	-	-	0.018	<0.001	0.02	0.013	0.197	<0.001
Grain filling	*Normal planting*											
	All	85.2±1.8	-8.1±0.1	14.9±0.3	0.79±0.02	0.51±0.02	61.2±1.6	-6.7±0.5	25.3±0.4	0.53±0.03	0.27±0.02	0.56±0.01
	Winter	90.3^{a}±1.9	-8.4^{b}±0.1	14.3^{b}±0.4	0.84^{a}±0.01	0.57^{a}±0.02	65.4^{a}±1.8	-8.1^{b}±0.5	24.5^{a}±0.4	0.60^{a}±0.03	0.33^{a}±0.02	0.59^{a}±0.01
	Facultative	71.7^{b}±2.9	-7.4^{a}±0.3	16.7^{a}±0.6	0.68^{b}±0.05	0.33^{b}±0.05	50.1^{b}±2.4	-3.1^{a}±1.1	27.4^{b}±0.5	0.33^{b}±0.05	0.13^{b}±0.03	0.47^{b}±0.02
	Late planting											
	All	92.7±1.3	-9.8±0.2	15.3±0.4	0.94±0.01	0.78±0.02	84.5±1.5	-14.8±0.5	25.3±0.3	0.84±0.02	0.63±0.02	0.69±0.01
	Winter	95.4^{a}±1.2	-9.9^{b}±0.2	14.7^{b}±0.4	0.95^{a}±0.01	0.85^{a}±0.02	92.5^{a}±1.1	-17.2^{b}±0.3	25.1^{b}±0.4	0.91^{a}±0.01	0.76^{a}±0.02	0.73^{a}±0.01
	Facultative	86.5^{b}±2.7	-9.6^{a}±0.3	16.5^{a}±0.5	0.91^{b}±0.01	0.61^{b}±0.05	66.5^{b}±2.1	-9.4^{a}±0.7	26^{a}±1	0.66^{b}±0.04	0.33^{b}±0.03	0.61^{b}±0.01
	ANOVA											
	PD	<0.001	<0.001	0.188	<0.001	<0.001	<0.001	<0.001	0.750	<0.001	<0.001	<0.001
	A	<0.001	<0.01	<0.01	<0.001	<0.001	<0.001	<0.001	<0.001	<0.001	<0.001	<0.001
	PD x A	<0.01	<0.01	0.051	0.978	<0.001	0.055	0.285	0.457	<0.001	0.682	0.286

Values are means ± standard error of the whole set (38) of genotypes and the winter (27) and facultative (11) subsets of genotypes. Levels of signification for the ANOVA: P < 0.05, P<0.01 and P<0.001. PD, Planting date; A, Attitude. Within each planting date, means exhibiting different letters are significantly different (P < 0.05) by t-student on independent samples. Sub-indices: g, ground; a, aerial.

Table 5: Effect of planting date (normal vs late) and genotype attitude (winter vs facultative) on ground and aerial temperature in both visits (at heading and grain filling), flag leaf and grains dry matter's carbon and nitrogen contents (%C and %N) and carbon and nitrogen isotopic composition ($\delta^{15}N$ and $\delta^{13}C$).

	Canopy temperature				Isotopic composition				
	Heading		Grain filling						
	CT.g (°C)	CT.a (°C)	CT.g (°C)	CT.a (°C)	$\delta^{13}C_{leaf}$ (‰)	$\delta^{15}N_{leaf}$ (‰)	C_{leaf} (%)	N_{leaf} (%)	$\delta^{13}C_{grain}$ (‰)
Normal planting									
All	26.1±0.1	26.9±0.11	28.9±0.9	27.7±0.2	-26.43±0.09	2.23±0.07	40.58±0.17	3.07±0.04	-25.66±0.06
Winter	25.9^{b}±0.1	26.8^{b}±0.1	28.7^{a}±0.2	27.4^{b}±0.2	-26.51^{b}±0.11	2.36^{a}±0.07	40.53^{a}±0.19	3.21^{a}±0.04	-25.76^{b}±0.07
Facultative	26.4^{a}±0.2	27.4^{a}±0.2	29.3^{a}±0.3	28.6^{a}±0.5	-26.24^{a}±0.15	1.90^{b}±0.13	40.72^{a}±0.33	2.70^{b}±0.07	-25.42^{a}±0.13
Late planting									
All	25.6±0.1	-	26.8±0.1	-	-28.76±0.07	2.94±0.06	40.19±0.24	2.76±0.06	-26.76±0.05
Winter	25.5^{a}±0.2	-	26.4^{b}±0.1	-	-28.52^{a}±0.07	3.08^{a}±0.07	40.22^{a}±0.28	2.96^{a}±0.06	-26.76^{a}±0.06
Facultative	25.8^{a}±0.2	-	27.7^{a}±0.3	-	-29.33^{b}±0.09	2.62^{b}±0.09	40.13^{a}±0.45	2.27^{b}±0.11	-26.77^{a}±0.08
ANOVA									
PD	<0.01	-	<0.001	-	<0.001	<0.001	0.194	<0.001	<0.001
A	<0.05	-	<0.001	-	<0.05	<0.001	0.987	<0.001	<0.05
PD x A	0.941	-	<0.05	-	<0.001	0.982	0.640	0.165	0.088

Values are means ± standard error of the whole set (38) of genotypes and the winter (27) and facultative (11) subsets of genotypes. Levels of signification for the ANOVA: P < 0.05, P<0.01 and P<0.001. PD, Planting date; A, Attitude. Within each planting date, means exhibiting different letters are significantly different (P < 0.05) by t-student on independent samples. Sub-indices: g, ground; a, aerial.

Table 6: Correlation coefficients of the linear regressions of wheat grain yield (GY) against days to heading, grain dry weight per spike (Grain weight spike^{-1}), number of grains per spike (grains spike^{-1}**)**, thousand grains weight (TGW), number of spikes per grown area (spikes m^{-2}), per planting date.

	Days to heading	**Grain weight spike^{-1}**	**Grains spike^{-1}**	**TGW**	**Nº spikes m^{-2}**
Normal planting					
All	0.435**	-0.285ns	0.130ns	-0.407*	0.276ns
Winter	-0.163ns	0.260ns	-0.010ns	0.266ns	-0.203ns
Facultative	0.264ns	-0.592ns	-0.070ns	-0.605ns	0.564ns
Late planting					
All	-0.430**	-	-	-	0.386*
Winter	-0.636**	-	-	-	0.429*
Facultative	0.076ns	-	-	-	0.472ns

Correlation values were calculate

*d across the whole (All) set (38) of genotypes or within the winter (27) and facultative (11) subsets of genotypes. (each genotypic value being the mean of three plots). Level of significance: ns, non-significant; *, $p < 0.05$; **, $p < 0.01$.*

Table 7: Correlations of RGB and multispectral indices assessed during heading and grain filling against GY within each planting date (Normal vs Late), per genotypes attitude (Winter vs Facultative) and by placement of sensors (Aerial vs Ground).

		RGB Indices											
		Hue.g	a*.g	b*.g	GA.g	GGA.g	Hue.a	a*.a	b*.a	GA.a	GGA.a	NDVI.g	NDV
Heading	*Normal planting*												
	All	0.058ns	0.222ns	-0.141ns	0.152ns	0.093ns	0.546**	0.495**	-0.538**	-0.537**	-0.517**	-0.100ns	0.2
	Winter	0.173ns	0.066ns	-0.109ns	0.160ns	0.100ns	0.363	0.392*	-0.357ns	-0.428*	-0.426*	-0.354ns	0.0
	Facultative	0.230ns	0.354ns	-0.556ns	0.191ns	0.173ns	0.658*	0.447ns	-0.562ns	-0.592ns	-0.565ns	0.256ns	0.2
	Late planting												
	All	-	-	-	-	-	0.159ns	0.590**	-0.486**	-0.147ns	0.170ns	-0.268ns	
	Winter	-	-	-	-	-	0.221ns	0.698**	-0.564**	-0.209ns	0.174ns	-0.329ns	
	Facultative	-	-	-	-	-	-0.080ns	-0.087ns	0.036ns	0.287ns	0.239ns	0.089ns	
Grain filling	*Normal planting*												
	All	0.568**	-0.538**	-0.338*	0.580**	0.525**	0.531**	-0.456**	-0.340*	0.527**	0.464**	0.560**	0.5
	Winter	0.141ns	0.078ns	-0.298ns	0.121ns	0.195ns	0.155ns	0.337ns	-0.235ns	-0.302ns	-0.034ns	0.057ns	0.1
	Facultative	0.529ns	-0.540ns	0.121ns	0.530ns	0.390ns	0.563ns	-0.807**	0.107ns	0.562ns	0.456ns	0.428ns	0.4
	Late planting												
	All	-0.077ns	0.294ns	-0.445**	-0.110ns	-0.109ns	-0.110ns	0.478**	-0.278ns	-0.160ns	-0.200ns	-0.222ns	-0.2
	Winter	0.089ns	0.462*	-0.551**	-0.119ns	0.023ns	-0.044ns	0.623**	-0.483*	-0.192ns	-0.202ns	-0.301ns	-0.2
	Facultative	0.282ns	-0.246ns	-0.052ns	0.232ns	0.245ns	0.035ns	-0.381ns	0.270ns	0.101ns	0.143ns	0.220ns	-0.0

*Correlation values were calculated across the whole (All) set (38) of genotypes or within the winter (27) and facultative (11) subsets of genotypes (each genotypic value being the mean of three plots). Abbreviations for subscripts are a (aerial) and g (ground). Levels of significance: ns, non-significant; *, P < 0.05; **, P < 0.01. Sub-indices: g, ground; a, aerial.*

Table 8: Correlations of ground-assessed (CT.g), and aerially assessed (CT.a) canopy temperature during heading and grain filling, carbon and nitrogen contents, carbon and nitrogen isotopic composition $\delta^{13}C$ and $\delta^{15}N$ in sampled flag leaves during grain filling and dry matter of mature grains, against GY within planting dates (Normal vs Late).

	Canopy temperature				Isotopic composition						
	Heading		Grain filling						Maturity		
	CT.g	CT.a	CT.g	CT.a	$\delta^{13}C_{leaf}$	$\delta^{15}N_{leaf}$	C_{leaf}	N_{leaf}	$\delta^{13}C_{grain}$	$\delta^{15}N_{grain}$	C_{grain}
Normal planting											
All	-0.198ns	-0.505**	-0.475**	-0.452**	-0.128ns	0.273ns	-0.161ns	0.498**	-0.553**	0.106ns	-0.040
Winter	0.307ns	-0.222	-0.274ns	-0.250ns	0.083ns	0.078ns	-0.098ns	0.057ns	-0.188ns	-0.089ns	-0.106
Facultative	-0.523ns	-0.606	-0.520ns	-0.393ns	-0.242ns	0.017ns	-0.240ns	0.347ns	-0.755*	0.088ns	0.079
Late planting											
All	-0.357*	-	0.150ns	-	-0.617**	-0.219ns	-0.053ns	-0.254ns	-0.591**	0.238ns	0.239
Winter	-0.583**	-	0.139ns	-	-0.692**	-0.160ns	-0.166ns	-0.330ns	-0.706**	0.357ns	0.215
Facultative	0.109ns	-	-0.161ns	-	-0.381ns	-0.152ns	0.382ns	0.370ns	0.037ns	-0.325ns	0.071

Correlation values were calculated across the whole (All) set (38) of genotypes or within the winter (27) and facultative (11) subsets of genotypes (each genotypic value being the mean of three plots). Abbreviations for subscripts are a (aerial) and g (ground). Levels

*of significance: ns, non-significant; *, P < 0.05; **, P < 0.01. Sub-indices: g, ground; a, aerial.*

Table 9: Multi-linear regression (stepwise) of grain yield (GY) as dependent variable, and the remote sensing traits (canopy RGB, multispectral vegetation indices and canopy temperature) measured from ground and aerial platforms and combined to carbon and nitrogen isotope composition ($\delta^{13}C$ and $\delta^{15}N$) as independent variables. $R^2_{adjusted}$, adjusted determination coefficient; RMSE, Root Mean Square Error; P-value, linear regression model significance.

		Grain yield predictions
Heading	*Normal planting*	
	All parameters	$Y=597.5 - 2421.4\ \%N_{grain} - 18738.6\ TCARIOSAVI.a + 5764.7\ EVI.a + 747.8\ \delta^{13}C_{leaf} - 1218.7\ \delta^{13}C_{grain}$
	Remote sensing	$Y= 1697.2 + 41.9\ Hue.a + 262.2\ b^*.g$
	Late planting	
	All parameters	$Y= -9614.1 - 559.1\ \delta^{13}C_{leaf} - 1702.1\ \%N_{grain} + 308.9\ a^*.a + 7133.4\ NDVI.g$
	Remote sensing	$Y= 8887.9 + 396.8\ a^*.a$
Grain filling	*Normal planting*	
	All parameters	$Y=2934.1 - 2942.2\ \%N_{grain} + 29594.9\ NDVI.a - 61017.9\ PRI.a - 673.9\ \delta^{15}N_{grain}$
	Remote sensing	$Y= 4118.2 + 14465.4\ CCI.a$
	Late planting	
	All parameters	$Y= -24815.4 - 617.7\ \delta^{13}C_{leaf} - 1812.9\ \%N_{grain} - 109.6\ b^*.a + 417.2\ \%C_{grain}$
	Remote sensing	$Y= 8154.9 + 333.6a^*.a$
Stable isotopes + nitrogen	*Normal planting*	
	Isotopes	$Y= -19.1 - 2389.2\ \%N_{grain} + 961.1\ \%N_{leaf} + 860.3\ \delta^{13}C_{leaf} - 1309.8\ \delta^{13}C_{grain}$
	Late planting	
	Isotopes	$Y= -9787.1 - 649.7\ \delta^{13}C_{leaf} - 1770.1\ \%N_{grain}$